DIPLOMARBEIT

Quasi-Normal Mode Expansion of the Scattering Matrix

ausgeführt am

Institut für Theoretische Physik
der Technischen Universität Wien

Institute for Theoretical Physics
Vienna University of Technology

unter der Anleitung von
Univ.-Prof. Dipl.-Ing. Dr. techn. Stefan Rotter
durch

Maximilian Korbinian Geismann

Datum

Unterschrift

Contents

Acknowledgements

I cordially thank my supervisor, Professor Stefan Rotter, who gave me the opportunity to write my master's thesis in theoretical physics even though my educational background is rooted elsewhere and always offered excellent support during my time in his group.

Furthermore, I would like to thank Faruk Salihbegović, whose work I continued and who helped me whenever he could through numerous discussions.

I also express my gratitude to Professor Thomas Weiss of the University of Stuttgart and his group for a memorable and prolific visit.

Additionally, I thank

- Barton Willis, from the Maxima mailing list for bringing the generalised Lambert-W function to my attention,
- István Mező, for responding to my enquiry about the r-Lambert function,
- Xiang Gao and Werner Nickel, for their time and willingness to discuss my work, and
- my colleagues and office neighbours for a delightful working environment and many shorter, but no less insightful, discussions.

Lastly, I thank my family and especially my wife to whom I am eternally indebted for their unconditional love and support.

Chapter 1.

Introduction

The scattering matrix, or S-matrix, is an incredibly useful tool in a wide range of applications. In simple terms, the S-matrix captures the relation between input and output of a scattering system. The information held by the S-matrix could be, e.g., the transmission of an electromagnetic wave propagating through a dielectric landscape or the angle of an electron's trajectory scattering off an atomic nucleus. Not only does the knowledge of the S-matrix enable to predict the output for an arbitrary 'excitation', it also allows to construct input states that precisely tune the response of the system in order to manipulate [1] or measure [2] certain quantities. A concrete example would be the recently demonstrated coherent perfect absorption in a random medium [3]: By measuring the S-matrix, the authors were able to find an input configuration that got completely absorbed by a sink inside the medium, i.e., there was no output.

The scattering matrix turns out to be strongly determined by the underlying resonances of a scattering system, which are also known as Quasi-Normal Modes (QNMs). We find these QNMs in the context of electrodynamics as well as quantum mechanics, when solving scattering problems with purely outgoing boundary conditions. As a compelling consequence, their eigenfrequencies or eigenenergies become complex, which might elude one's physical intuition, especially, as they cause the QNM-fields to diverge far away from the scatterer. Yet, these states are the key to a better understanding of complex scattering systems: it is well known, that QNMs can be linked to isolated resonances in scattering spectra, cf. [4]. In the diffusive regime, however, the spectra become a crowded superposition of overlapping resonances and it is not clear how to exactly reconstruct them in the QNM-picture. Being able to do so would lead to a compact description of complex scattering systems which could ultimately be used to express the entire S-matrix.

In this work, we investigate various QNM-expansions of the S-matrix. The complex QNM-energies coincide with the poles of the S-matrix, which, in turn, are directly connected to resonances of the real scattering spectra. As a consequence, all of the methods presented here are based on pole expansions. Ideally, the only parameters required can be derived from the QNMs. The main difficulty

of this ansatz is the calculation of the correct residues, beside other issues like background contributions or the proper normalisation of the QNMs. The reward for overcoming these obstacles is a semi-analytical formula for the S-matrix which has many advantages: Once the QNMs are calculated, such a formula would beat any conventional fully numerical routine in terms of computation time, because they have to be re-run for every desired frequency or energy point in the spectrum. More importantly, such an S-matrix expansion would yield an efficient and physical description of complex scattering phenomena that could not only be leveraged to improve control over complex scattering systems but also to further explore their intriguing properties.

Chapter 2.

The Scattering Matrix

The scattering matrix or S-matrix is the central tool for describing scattering processes. In quantum mechanics it was introduced by Heisenberg in 1943 as the 'characteristic matrix' for scattering problems [5]. However, the S-matrix captures a quite general concept: given some input vector α^{in} that describes an incoming wave[1], may that be an electronic wavefunction or a classical electromagnetic field, the S-matrix yields the outgoing wave, represented by the output vector α^{out}, by multiplying α^{in} from the right

$$\alpha^{\text{out}} = S\alpha^{\text{in}} \,. \tag{2.1}$$

As such it appears in a wide variety of fields ranging from nuclear physics [6] to electronic transport [7], optics [8] and even acoustics [9]. The ability to measure or calculate the S-matrix is invaluable for an abundance of applications. In optics, for example, a breakthrough [10] demonstrated how to measure the transmission matrix—a submatrix of the S-matrix—of complex media which facilitated the means to study focusing and imaging in such media [11]. Similarly, the S-matrix allows to determine optimal input configurations for controlling branched flow [12], micro-manipulation [1] or maximum information measurements [2].

The present work focuses on the resonances of scattering systems and their potential to represent any S-matrix in a compact and semi-analytical form. Such a 'resonance expansion' could speed up the numerical calculation of the S-matrix considerably and is the key to a better understanding of scattering processes applicable to all of the above examples. But before we concern ourselves with such matters, we will establish some basic properties of the S-matrix.

2.1. Scattering on the Potential Barrier

Let us illustrate how the S-matrix is applied on a classic example: consider the quantum mechanical potential barrier in one dimension, Figure 2.1. The incoming

[1] The vector's entries are the expansion coefficients of the wave in some basis, e.g., complex amplitudes of a Fourier-series.

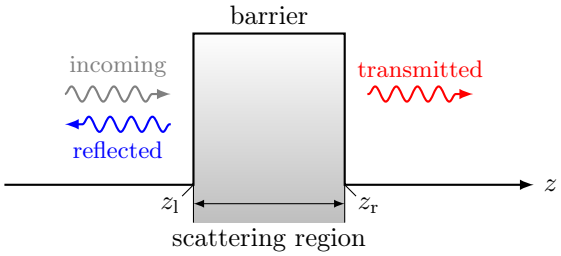

Figure 2.1.: Scattering on a potential barrier in one dimension: An incoming wave from the left (grey) is scattered on the barrier. The scattered waves, i.e., the reflected (blue) and the transmitted (red) parts, propagate freely away from the barrier.

plane wave propagates freely until it hits the barrier where it is partially reflected and partially transmitted. Both, the reflected and transmitted part, then propagate freely away from the barrier. In the plane wave basis we have two input 'channels'; one for incoming waves from the left and one for incoming waves from the right:

$$\psi_\mathrm{l}^\mathrm{in}(z) = \alpha_\mathrm{l}^\mathrm{in} \exp(ikz)\,, \quad \psi_\mathrm{r}^\mathrm{in}(z) = \alpha_\mathrm{r}^\mathrm{in} \exp(-ikz)\,.$$

Analogously, we have two output channels carrying plane waves away from the barrier,

$$\psi_\mathrm{l}^\mathrm{out}(z) = \alpha_\mathrm{l}^\mathrm{out} \exp(-ikz)\,, \quad \psi_\mathrm{r}^\mathrm{out}(z) = \alpha_\mathrm{r}^\mathrm{out} \exp(ikz)\,.$$

So, every channel has a designated direction of propagation as well a designated side or port. The complex amplitudes of the waves carried in each channel are the entries of the input and output vectors

$$\alpha^\mathrm{in} = \begin{pmatrix} \alpha_\mathrm{l}^\mathrm{in} \\ \alpha_\mathrm{r}^\mathrm{in} \end{pmatrix}, \quad \alpha^\mathrm{out} = \begin{pmatrix} \alpha_\mathrm{l}^\mathrm{out} \\ \alpha_\mathrm{r}^\mathrm{out} \end{pmatrix}. \tag{2.2}$$

Since the wavenumber k is the same for all waves, we can express the outgoing amplitude, say, $\alpha_\mathrm{l}^\mathrm{out}$ by adding the fraction of $\alpha_\mathrm{l}^\mathrm{in}$ that got reflected to the fraction of $\alpha_\mathrm{r}^\mathrm{in}$ that got transmitted:

$$\alpha_\mathrm{l}^\mathrm{out} = r_{\mathrm{l}\leftarrow\mathrm{l}}\, \alpha_\mathrm{l}^\mathrm{in} + t_{\mathrm{l}\leftarrow\mathrm{r}}\, \alpha_\mathrm{r}^\mathrm{in}\,,$$

where $r_{\mathrm{l}\leftarrow\mathrm{l}}$ is the reflection amplitude from left to left and $t_{\mathrm{l}\leftarrow\mathrm{r}}$ is the transmission amplitude from right to left. Following this logic we obtain the S-matrix as

$$S = \begin{pmatrix} r_{\mathrm{l}\leftarrow\mathrm{l}} & t_{\mathrm{l}\leftarrow\mathrm{r}} \\ t_{\mathrm{r}\leftarrow\mathrm{l}} & r_{\mathrm{r}\leftarrow\mathrm{r}} \end{pmatrix}. \tag{2.3}$$

Keep in mind that reflection and transmission *amplitudes* are complex quantities. The terms 'reflection' and 'transmission' (without 'amplitude'), denoted R and T, respectively, refer to the reflected or transmitted fraction of the intensity. Thus,

$$R_{\mathrm{l}\leftarrow\mathrm{l}} = |r_{\mathrm{l}\leftarrow\mathrm{l}}|^2\,, \quad T_{\mathrm{l}\leftarrow\mathrm{r}} = |t_{\mathrm{l}\leftarrow\mathrm{r}}|^2\,,$$
$$T_{\mathrm{r}\leftarrow\mathrm{l}} = |t_{\mathrm{r}\leftarrow\mathrm{l}}|^2\,, \quad R_{\mathrm{r}\leftarrow\mathrm{r}} = |r_{\mathrm{r}\leftarrow\mathrm{r}}|^2\,.$$

2.1.1. Unitarity

The S-matrix of the potential barrier must be unitary as can be shown as follows: In quantum mechanics and electrodynamics (if we consider the scalar Helmholtz equation), the flux $\mathbf{J}(\mathbf{r})$, i.e., probability density or current density, is found to be

$$\mathbf{J}(\mathbf{r}) \propto \mathrm{Im}\{\psi^*(\mathbf{r})\,\nabla\psi(\mathbf{r})\}\,. \tag{2.4}$$

Since there is no gain or loss in the barrier[2]—meaning there are no sinks or sources which absorb or generate flux—the incoming flux must equal the outgoing flux at the boundary of the scattering region in the outwards pointing direction:

$$J_{\mathrm{l}}^{\mathrm{in}}(z_{\mathrm{l}}) - J_{\mathrm{r}}^{\mathrm{in}}(z_{\mathrm{r}}) = J_{\mathrm{l}}^{\mathrm{out}}(z_{\mathrm{l}}) - J_{\mathrm{r}}^{\mathrm{out}}(z_{\mathrm{r}})\,.$$

By plugging the plane wave basis $\psi_{\mathrm{l}}^{\mathrm{out}}$, $\psi_{\mathrm{r}}^{\mathrm{out}}$, $\psi_{\mathrm{l}}^{\mathrm{in}}$ and $\psi_{\mathrm{r}}^{\mathrm{in}}$ into (2.4), we arrive at $|\alpha_{\mathrm{l}}^{\mathrm{in}}|^2 + |\alpha_{\mathrm{r}}^{\mathrm{in}}|^2 = |\alpha_{\mathrm{l}}^{\mathrm{out}}|^2 + |\alpha_{\mathrm{r}}^{\mathrm{out}}|^2$. Switching to vector notation, cf. Equation (2.2), and using (2.1) we get:

$$\begin{aligned}
\left(\alpha^{\mathrm{in}}\right)^\dagger \alpha^{\mathrm{in}} &= \left(\alpha^{\mathrm{out}}\right)^\dagger \alpha^{\mathrm{out}} \\
&= \left(S\alpha^{\mathrm{in}}\right)^\dagger S\alpha^{\mathrm{in}} \\
\left(\alpha^{\mathrm{in}}\right)^\dagger \alpha^{\mathrm{in}} &= \left(\alpha^{\mathrm{in}}\right)^\dagger S^\dagger S\alpha^{\mathrm{in}} \\
\Rightarrow S^\dagger S &= \mathbb{1}\,.
\end{aligned} \tag{2.5}$$

Thus, the S-matrix is unitary which implies that $R + T = 1$, meaning there is no fraction of the intensity that gets lost. Also, assuming that there is no gain or loss, unitarity holds for more general systems as well.

2.1.2. Transposition Symmetry

Usually, the S-matrix is transposition symmetric[3]. In the case of the potential barrier we can reveal this fact by inspecting the symmetry of the system: If we flipped the z-axis in Figure 2.1 and sent the incoming wave from the right instead

[2] Mathematically, gain or loss could be introduced by making the potential complex.
[3] A matrix A is symmetric or transposition symmetric if $A = A^T$.

of the left, we could not make out a difference to the original figure (disregarding textual labels). Consequently, scattering from one side cannot be any different from scattering from the other side:

$$\begin{aligned} r_{\mathrm{l}\leftarrow\mathrm{l}} &= r_{\mathrm{r}\leftarrow\mathrm{r}} \\ t_{\mathrm{r}\leftarrow\mathrm{l}} &= t_{\mathrm{l}\leftarrow\mathrm{r}} \\ \Rightarrow S &= S^T \,. \end{aligned}$$

One could be tempted to attribute the transposition symmetry to the mirror or rotational symmetry (rotation by 180° around the z-axis) of this problem. However, $S = S^T$ holds even for *asymmetric* systems where left and right can be distinguished; the complex waveguide presented in Section 4.1.2 being such an example. In these cases, one could argue that time-reversal symmetry is responsible: a scattering system is symmetric under time-reversal if for all input-output pairs, related through $\alpha^{\mathrm{out}} = S\alpha^{\mathrm{in}}$, the time-reversed amplitudes are related by the same S-matrix [13] which leads to:

$$\begin{aligned} (\alpha^{\mathrm{in}})^* &= S(\alpha^{\mathrm{out}})^* \\ (\alpha^{\mathrm{in}})^* &= S(S\alpha^{\mathrm{in}})^* \\ \Rightarrow SS^* &= \mathbb{1} \,. \end{aligned} \tag{2.6}$$

But time-reversal symmetry implies unitarity of the S-matrix [14], because otherwise $\alpha^{\mathrm{out}} = S\alpha^{\mathrm{in}}$ and $(\alpha^{\mathrm{in}})^* = S(\alpha^{\mathrm{out}})^*$ could not hold simultaneously[4]. Combining (2.6) with unitarity we obtain:

$$\begin{aligned} SS^* &= \mathbb{1} = SS^\dagger \\ SS^* &= S(S^T)^* \\ \Rightarrow S &= S^T \,. \end{aligned}$$

As we see, transposition symmetry is tied to the common notion of time-reversibility. In reality, however, transposition symmetry is a consequence of an even more fundamental property: Reciprocity. A thorough discussion can be found in [15] which describes reciprocity as the symmetry of the scattering amplitude under exchange of source and detector. The formal definition of reciprocity employs an anti-unitary operator; such as the time-reversal operator. However, there are other anti-unitary operators that fulfil the reciprocity conditions given in [15], and thus $S = S^T$ holds even for systems that are not time-reversal symmetric, i.e., systems with gain or loss. Reciprocity and time-reversal symmetry hold for all of the systems we study in this work; non-reciprocity is normally a feature reserved for 'exotic' problems.

[4] A unitary operator A preserves the metric of any state it is acting on, $||Ax|| = ||x||$. If the S-matrix was not unitary, we could not swap incoming and outgoing amplitudes, as their metrics—their 'lengths'—would not match in general.

2.2. S-Matrix for Waveguide Structures

The previous section covered the essential properties of the S-matrix in the simple setting of the one-dimensional potential barrier. But its scope is limited and fails to capture other important aspects of scattering problems. For this reason, let us turn our attention to a more realistic geometry: The two-dimensional waveguide.

Rectangular 2D waveguides are an important experimental platform on which plenty of phenomena have been demonstrated and examined [1, 3, 12, 16]. In an ideal representation, such a waveguide consists of two infinite and parallel 'hard walls', i.e., an infinite potential or a perfectly conducting metallic layer. In either case, the wavefunction or the field cannot penetrate the hard wall and must be zero at the boundary. The scattering region is embedded in the 'centre' of the waveguide between the walls and typically consists of cylindrical scatterers because they are conveniently realised in our experimental setup. See Figure 4.1 for an example geometry.

Similar to the 1D case, we distinguish between left and right channels that are either incoming or outgoing. The modes of the 2D waveguide carried by these channels behave like plane waves in z-direction with wavenumber κ. There is, however, a transversal component K_n in y-direction so that $\kappa_n = \sqrt{k^2 - K_n^2}$, with k the magnitude of the (total) wave vector. Of course, K_n can only assume values that lead to a vanishing field on the waveguide walls: if we choose the y-origin to coincide with the upper wall and assume a distance of L between the walls, then $K_n = 2\pi n/L$, where n is some positive integer, and the waveguide modes take the form

$$\psi_n(y, z; k) = \underbrace{\frac{\alpha_n}{\sqrt{\kappa_n(k)}}}_{=\widetilde{\alpha}_n} \sqrt{\frac{2}{L}} \sin(K_n y/2) e^{i\kappa_n(k)z} \quad n = 1, 2, \dots,$$

where $\widetilde{\alpha}_n = \alpha_n/\sqrt{\kappa_n(k)}$ is the flux-normalised complex amplitude of the mode (discussed below) and $\sqrt{2/L}$ normalises the transverse profile to unity. For a given k, each channel can carry a limited amount of *open* modes, i.e., modes for which $k \geq K_n = 2\pi n/L$. For $k < K_n$, κ would become imaginary, corresponding to *closed* modes, i.e., evanescent modes, which do not matter asymptotically[5].

The input and output vectors are defined analogously to (2.2) but contain as many entries as open modes per side:

$$\alpha^{\text{in/out}} = \left(\alpha_{\text{l1}}^{\text{in/out}}, \alpha_{\text{l2}}^{\text{in/out}}, \dots, \alpha_{\text{r1}}^{\text{in/out}}, \alpha_{\text{r2}}^{\text{in/out}}, \dots\right)^T.$$

As a consequence the S-matrix, that relates open incoming to open outgoing modes, increases its size as more modes become energetically available with in-

[5] One can generalise the S-matrix to work with evanescent fields, see [13].

creasing k: $2 > kL/(2\pi) \geq 1 \Rightarrow S(k) \in \mathbb{C}^{2\times 2}$, $3 > kL/(2\pi) \geq 2 \Rightarrow S(k) \in \mathbb{C}^{4\times 4}$ and so on. For convenience we define a maximum amount of open modes and keep the dimensions of the S-matrix fixed. Entries related to inactive modes (depending on k) are set to zero. Still, the S-matrix assumes the form (2.3), the entries, however, are now matrices:

$$S = \begin{pmatrix} r^{\text{left}} & t^{\text{right}} \\ t^{\text{left}} & r^{\text{right}} \end{pmatrix}$$

$$r^{\text{left/right}} = \begin{pmatrix} r_{11}^{\text{left/right}} & r_{12}^{\text{left/right}} & \dots \\ r_{21}^{\text{left/right}} & r_{22}^{\text{left/right}} & \dots \\ \vdots & \vdots & \ddots \end{pmatrix} \quad t^{\text{left/right}} = \begin{pmatrix} t_{11}^{\text{left/right}} & t_{12}^{\text{left/right}} & \dots \\ t_{21}^{\text{left/right}} & t_{22}^{\text{left/right}} & \dots \\ \vdots & \vdots & \ddots \end{pmatrix}.$$

The superscripts 'left' and 'right' correspond, on the one hand, to the position of the column and, on the other hand, to the port from which the scattering originated. Again, the reflection and transmission will be the absolute-square of the reflection and transmission amplitudes; $R_{ij}^{\text{left/right}} = |r_{ij}^{\text{left/right}}|^2$ and $T_{ij}^{\text{left/right}} = |t_{ij}^{\text{left/right}}|^2$.

In contrast to the potential barrier, one channel carrying a certain mode can scatter into channels carrying different modes, i.e., modes with a different value of K_n and thus $\kappa_n(k)$. This circumstance is called *mode-mixing* and manifests itself in non-zero off-diagonal elements of the submatrices $r^{\text{left/right}}$ and $t^{\text{left/right}}$. The possibility of mode-mixing has consequences for the unitarity relation: The incoming flux must still equal the outgoing flux but this time we have to take contributions from other modes into account (and integrate over the interface, cf. [13]). This leads to

$$\begin{aligned} \sum_i \kappa_i (|\widetilde{\alpha}_{\text{l}i}^{\text{in}}|^2 + |\widetilde{\alpha}_{\text{r}i}^{\text{in}}|^2) &= \sum_j \kappa_j (|\widetilde{\alpha}_{\text{l}j}^{\text{out}}|^2 + |\widetilde{\alpha}_{\text{r}j}^{\text{out}}|^2)\,, \\ \sum_i (|\alpha_{\text{l}i}^{\text{in}}|^2 + |\alpha_{\text{r}i}^{\text{in}}|^2) &= \sum_j (|\alpha_{\text{l}j}^{\text{out}}|^2 + |\alpha_{\text{r}j}^{\text{out}}|^2)\,, \\ \Rightarrow S^\dagger S &= \mathbb{1}\,, \end{aligned}$$

where the last line follows from the same steps taken in (2.5). As we see, the flux normalisation is necessary to get rid of the κ_i terms and obtain unitarity of the S-matrix.

2.3. Calculating the S-Matrix Numerically

Typically we partition space into the *scattering region*, where the actual interaction of the incoming wave and the scatterer takes place, and the *asymptotic*

region outside the scattering region where incoming and outgoing/scattered waves propagate freely. This partition is an important concept that allows to confine the scattering problem to a finite space through appropriate boundary conditions. Consequently, it enables us to solve scattering problems numerically as we will demonstrate for the one-dimensional case. The concept is straightforwardly extended to two dimensions as discussed in [17].

First, we need to discretise the scattering region in space with a finite amount of sampling points z_j, with $j = 1, 2, ..., N$, spaced equidistantly apart by Δz. We consider systems that can always be cast into a Hamiltonian H with a local potential $V(z)$ and so the discretisation procedure yields the well-known tri-diagonal matrix H_D approximating the Hamiltonian inside the scattering region, i.e., $H \triangleq H_D$ [7, 17]:

$$H_D = -t \begin{pmatrix} \ddots & & & & & \\ 1 & -2 & 1 & & & \\ & 1 & -2 & 1 & & \\ & & 1 & -2 & 1 & \\ & & & & \ddots \end{pmatrix} + \begin{pmatrix} \ddots & & & & & \\ 0 & V(z_j) & 0 & & & \\ & 0 & V(z_{j+1}) & 0 & & \\ & & 0 & V(z_{j+2}) & 0 & \\ & & & & \ddots \end{pmatrix},$$

where $t = 1/(2\Delta z^2)$ is the hopping parameter; a measure of the coupling strength between points.

So far, H_D represents a closed system, namely, the system that emerges if the scattering region was enclosed with hard walls. In order to 'open' H_D and connect it to the asymptotic region we introduce open boundary conditions: since the solutions must propagate like plane waves outside the scattering region, the values of any solution at the boundary on the inside ($j = 1$ and $j = N$) are related to the outside ($j = 0$ and $j = N + 1$) by:

$$\psi_0 = e^{ik\Delta z}\psi_1\,,$$
$$\psi_{N+1} = e^{ik\Delta z}\psi_N\,,$$

where the phase term $\exp(ik\Delta z)$ is the phase that a plane wave would acquire propagating over a distance of Δz. These boundary conditions are incorporated into H_D to yield the *effective Hamiltonian*, H_{eff}, which describes the finite but open system, as follows:

$$H_{\text{eff}} = H_D + B\,, \tag{2.7}$$
$$B = -t \begin{pmatrix} e^{ik\Delta z} & & \\ & \ddots & \\ & & e^{ik\Delta z} \end{pmatrix}.$$

Next, we introduce the (discrete) *effective Green's function*, G_{eff}, which is the inverse of $E - H_{\text{eff}}$:

$$\begin{aligned}(E - H_{\text{eff}})G_{\text{eff}} &= \mathbb{1}/\Delta z \\ \Rightarrow G_{\text{eff}} &= ((E - H_{\text{eff}})\Delta z)^{-1} ,\end{aligned}$$

where E is the energy and the factor $1/\Delta z$ appears due to the discrete nature of the operators and the requirement that integration over one spatial coordinate yields unity[6]. By 'integration' we mean a Riemann sum, $\int f(z)\mathrm{d}z \triangleq \sum_j f(z_j)\Delta z$.

The effective Green's function specifies how waves propagate inside the scattering region, i.e., how they are scattered. Defining appropriate coupling operators, $W^\dagger$ and W, allows us to couple an incoming wave into the system, let it scatter by applying G_{eff}, and finally couple it to outgoing waves in the asymptotic region. In this way we can determine all the entries of the S-matrix by sending an incoming wave through every channel. Executing this idea in formulae, we find that

$$W = \begin{pmatrix} \sqrt{\sin(k\Delta z)}/\Delta z & 0 \\ 0 & 0 \\ \vdots & \vdots \\ 0 & \sqrt{\sin(k\Delta z)}/\Delta z \end{pmatrix} ,$$

where the dimension of W is $N \times N_c$, with N_c the number of channels (here $N_c = 2$ for left and right), and ultimately obtain the effective Hamiltonian formula for the S-matrix[7]:

$$\boxed{S = \mathbb{1} - iW^\dagger G_{\text{eff}} W} . \tag{2.8}$$

The numerical implementation of Equation (2.8) is straightforward for simple systems: we construct H_D, choose an energy E, run a matrix inversion routine to obtain G_{eff} and multiply the coupling matrices $W^\dagger$ and W, and substitute the resulting matrix $W^\dagger G_{\text{eff}} W$ into (2.8) to get the S-matrix at energy E. For complex systems, the direct inversion of $E - H_{\text{eff}}$ becomes infeasible and other methods must be employed to obtain G_{eff}, like the iterative scheme proposed in [18].

A final remark regarding the discrete system: the quantum mechanical dispersion relation $E = k^2/2$, where we assumed $\hbar = m = 1$, translates into

$$E = 2t(1 - \cos(k\Delta z)) .$$

Of course, both forms are asymptotically equivalent as $k\Delta z \to 0$. Therefore, one should choose Δz according to the largest possible value of k such that $k\Delta z$ stays small and the discrete system is a good approximation of the real and continuous system.

[6] This stems from the fact that in the continuous case $(E - H)G(z, z') = \delta(z - z')$ and $\int \delta(z - z')\mathrm{d}z = 1$.

[7] The detailed derivation can be found in Appendix A.

Chapter 3.

Quasi-Normal Modes

Closed or conservative systems, i.e., Hermitian systems, have discrete and real-valued eigenenergies E_m or eigenfrequencies ω_m. The corresponding eigenstates are the *normal modes*: imagine a harmonic oscillator resonating at its eigenfrequency with time-dependence $\propto \exp(-i\omega_m t)$ for eternity. If we introduce damping, however, the resulting oscillation will decay exponentially in time, with time-dependence $\propto \exp(-i\omega_m t)\exp(-\Gamma_m t/2)$, because it continuously dissipates energy. This damped state assumes the same time dependence as a normal mode if we define its eigenfrequency to be complex, $\widetilde{\omega}_m = \omega_m - i\Gamma_m/2$. Due to this analogy, we call such a dissipative or decaying state a *Quasi-Normal Mode* (QNM)[1].

In a more general context, the damping of the harmonic oscillator corresponds to opening a closed system, which will always coincide with the scattering region in this work, by coupling it, e.g., to free space or waveguide leads. As a consequence, the real energies or frequencies are shifted onto the complex plane. In [23], this phenomenon is discussed in regard to the density of states (DOS): a closed system exhibits a 'discrete' DOS with Dirac deltas positioned at the eigenenergies, i.e., the normal modes. After opening the system, each Dirac delta will broaden to yield a continuous DOS and might slightly shift its position. The resulting line shape is Lorentzian which is described by the 'projection' of the squared magnitude of a simple pole located at the shifted energy $\widetilde{E}_m$ in the complex plane:

$$\delta(E - E_m) \to \left| \frac{1}{E - \widetilde{E}_m} \right|^2 .$$

In Figure 3.1 we see that the imaginary part of $\widetilde{E}_m$, $\widetilde{E}''_m := \mathrm{Im}\{\widetilde{E}_m\}$, determines the width of the line shape: the larger it is, the broader the Dirac delta becomes. Since $\Gamma_m = -2\widetilde{E}''_m$, an increased line width translates into a larger damping factor in the time domain, meaning that the energy initially stored inside the system dissipates more quickly. Consider, for instance, an electron occupying some eigenstate inside a closed system: after opening the system the electron's wavefunction will decay

[1] QNMs have also been called *decaying states* [19], *resonant states* [20], *leaky modes* [21] or *quasiguided modes* [22].

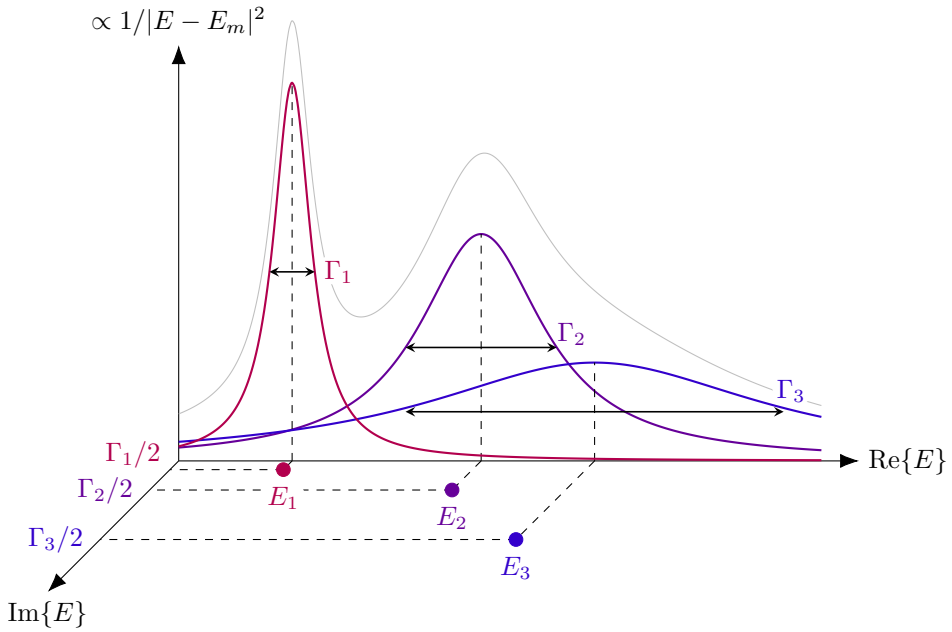

Figure 3.1.: Several Lorentzian peaks with different widths and positions arising from poles (dots) in the complex E-plane. The imaginary part of the poles, $\Gamma_m/2$, determines the line width, Γ_m, i.e., the full-width-half-maximum, indicated by the double arrows. The light grey curve is a toy-spectrum obtained by summing over all Lorentzians, demonstrating the principle of a pole based reconstruction.

and eventually 'escape' [19]. The electron's life time inside the system is thus inversely proportional to the line width and consequently the imaginary part of its shifted eigenenergy. In general, the real-part might be altered as well (conversely to the damped oscillator example), effectively shifting the position of the Lorentzian peak.

We see that, even though the DOS of an open system is continuous, it can be described by a discrete set of simple poles. These poles originally lie on the real axis—in form of Dirac deltas—located at the real eigenenergies of the closed system, but by opening the system they get shifted onto the complex plane, where the imaginary part of the shift is physically interpreted as the inverse lifetime. These *shifted eigenstates* are the QNMs.

The principle of representing Lorentzian peaks with simple poles and thus with QNMs, is very powerful and works not only for the DOS but also for transmission

and reflection spectra, as demonstrated, for example, by the prominent Breit-Wigner formula from nuclear physics [4]. From this perspective, each resonance, i.e., each peak of the spectrum, is linked to a QNM. Finding such a representation of the S-matrix, which is the subject of the next chapter, would allow to interpret even complex scattering spectra on a physical basis provided by the QNMs.

3.1. Properties

We introduced the QNMs as decaying states with complex energies or frequencies. Assuming a time dependence $\exp(-i\widetilde{\omega}_m t)$, it follows that the imaginary part must be less than zero. The same holds for the wave number[2], k_m, and thus the spatial dependence, $\exp(ikz)$, is exponentially divergent outside the originally closed scattering region. A normalisation of the QNMs in the conventional sense is therefore impossible. Still, a proper normalisation can be derived rigorously, see Section 4.3.4 or [24, 25]. Intuitively, the divergence can be thought of as the tail of a previous excitation that already left the system a 'long' time ago. The almost vanishing residue of this excitation is thought to be renormalised or 'amplified' so that its peak, located far away from the scattering region, seems to become infinite.

How can we calculate the QNMs? The normal modes are easily obtained by solving the typical eigenvalue problem of the Hamiltonian H:

$$H\psi = E\psi\,. \tag{3.1}$$

Formally, we open the system by introducing Boundary Conditions (BCs) that force the solution to be freely propagating outside the scattering region. We already discussed this procedure in the previous chapter for the discrete case, Equation (2.7). In the continuous and one-dimensional case, the BC reads

$$\frac{\mathrm{d}\psi(z)}{\mathrm{d}z}\,|_{z=z_0} = ik\psi(z_0)\,, \tag{3.2}$$

which is obtained from (2.7) by letting Δz go to zero [17]. Note, that the BC is defined on the interface between the scattering region and the asymptotic region at $z = z_0$. Integrating this BC into (3.1) leads to the generalised eigenvalue problem

$$H(E)\psi = E\psi\,, \tag{3.3}$$

with an *energy-dependent* Hamiltonian, which renders this problem non-linear. The QNMs arise as the solutions of (3.3) for *purely outgoing* BCs because of

[2] In electrodynamics this is obvious due to the linear dispersion relation $k = \omega/c$. In quantum mechanics $k = \sqrt{2E}$, but the imaginary part is still less than zero for one of the two branches. The other branch contains 'incoming' QNMs with the same energy which will not play a role in this work.

their dissipative nature. Purely outgoing means that there is no incoming wave. This might seem counter-intuitive at first, as the field appears to be generated inside the scattering region even though we did not add any sources. But due to the connection between QNMs and normal modes, we can argue that the source is a bound state that escaped the system. Solving Equation (3.3) numerically for complex systems is non-trivial but there exist several techniques [26]. Also, QNMs come in pairs [27]: if k_m is a QNM eigenvalue, so is $-k_m^*$.

Lastly, we shall note, that there is a similar eigenvalue problem for the effective Hamiltonian, H_{eff} (see Section 2.3 and Appendix A), that fixes the wavenumber found in the BC (3.2) to an arbitrary but real value k_0 [28, 29]. The effective Hamiltonian containing the BCs will thus be fixed, i.e., energy-*independent* and we obtain the linear but non-Hermitian eigenvalue problem

$$H_{\text{eff}}(E_0)\psi = E\psi\,.$$

The solutions are the so-called *Constant-Flux* (CF) states [30]. They are only defined inside the scattering region, as is H_{eff}. Due to the fixed BC we can, however, treat them as plane waves in the exterior, i.e., CF states do not diverge[3]. Even though they form a biorthogonal basis in the interior, they are not solutions to the underlying differential equation and must be calculated anew for each energy E_0.

3.2. Quasi-Normal Modes as Poles of the S-matrix

The fact, that QNMs are non-zero and outgoing solutions to a problem without any incoming wave has interesting consequences for the S-matrix at a QNM-wavenumber k_m: We can multiply the zero input vector and still produce a non-zero output. We conclude that the S-matrix must have a pole at each k_m, with the rationale being that only infinity times zero yields something non-zero. Going back to the effective Hamiltonian formula for the S-matrix, Equation (2.8), we see that the poles originate from the effective Green's function because the coupling matrices W and $W^\dagger$ are free of poles. This is also true for the 'real' Green's function of the system and leads to its QNM-expansion or Mittag-Leffler expansion [31] that will be central to the pole expansion presented in the next chapter.

Analogous to the pole picture of the DOS from the beginning of this chapter, we ultimately seek to express the S-matrix in terms of QNMs; one for each resonance in the transmission and reflection spectra. Mathematically, this corresponds to finding a pole expansion of the S-matrix. Contrary to a Laurent series, which is a

[3] Setting k, appearing in the BC, to a complex value, will cause the CF states to diverge. In fact, setting k to one of the k_m of the QNMs will cause exactly one CF state to be equal to the according QNM. All other CF states of the eigenbasis of H_{eff} differ from the rest of the QNMs, even though they might be similar [30].

power series around a *single* pole, we will employ the Mittag-Leffler-type expansion [32] that takes all poles into account. Furthermore, as the S-matrix is an operator, we will need to find residues in operator form. Such a representation is attractive since it allows physical insights into the scattering problem and, as discussed in the next chapter, enables an efficient numerical computation of the S-matrix.

In order to represent the S-matrix over the desired spectral interval, i.e, the range of interest for k, ω or E, we need to incorporate all those QNMs whose real parts lie within said interval: each QNM 'resolves' a single resonance or peak of the spectrum where the position is determined by the real part of the complex eigenenergy or eigenfrequency. Nonetheless, for an adequate representation one must include additional QNMs lying outside (but close to) the interval. This concerns, especially, broad resonances with a large imaginary part as their long tails might extend into the interval. Occasionally, one introduces a smooth, i.e, slowly varying, background term to capture the contributions of these broad resonances located within as well as outside the interval. This background is not clearly defined as there is no general rule to determine what qualifies as a broad resonance and thus which QNMs to include. But even if all resonances would be included in the pole expansion, there might be a non-resonant background containing no poles as shown in the next chapter, Section 4.3. Either way, the background term is usually calculated through a fitting routine which requires the values of the S-matrix at a sufficient amount of points throughout the spectrum. Even though this can be achieved by conventional numerical methods, it would be desirable to represent the S-matrix through a QNM-expansion without any fit parameters.

3.3. Poles and Zeros in the S-Matrix Eigenbasis

So far we established the connection between QNMs and poles of the S-matrix. Additionally, QNMs are linked to the zeros of the S-matrix: imagine a system in a state comprised of a single QNM. Initially, there is only outgoing flux. However, after time reversing the QNM[4], which yields another valid state if we assume time-reversal symmetry, all outgoing flux is reversed and there is only *incoming* flux. Seen in the context of scattering, the S-matrix for this configuration is said to have a 'zero' since we send something in but nothing goes out. This does *not* mean that the S-matrix has all-zero entries: the 'zero' only occurs for a certain energy or frequency and a particular incoming wave, namely an eigenstate of the S-matrix.

In order to better understand this circumstance, let us diagonalise the S-matrix for a one-dimensional and symmetric system like the potential barrier from the previous chapter or the Fabry-Pérot cavity presented in Section 4.3.5. The exact form is insignificant here. The only relevant property is that the QNMs are either

[4]If the QNM-wavenumber is k_m, then the time-reversed wavenumber will be $-k_m$.

even or odd functions[5]; this is a direct consequence of the symmetry of the system. Furthermore, the S-matrix must be unitary and transposition symmetric as there is no loss or gain and reciprocity holds. Consequently, the S-matrix has even and odd eigenstates. This can immediately be checked as the S-matrix is a two-by-two matrix of the form

$$S(k) = \begin{pmatrix} r(k) & t(k) \\ t(k) & r(k) \end{pmatrix} , \tag{3.4}$$

with the even eigenvalue $e(k) = r(k) + t(k)$ and eigenstate $\mathbf{v}_e = (1,1)^T$ and the odd eigenvalue $o(k) = r(k) - t(k)$ and eigenstate $\mathbf{v}_o = (1,-1)^T$. After the diagonalisation the S-matrix will be

$$\widetilde{S}(k) = \begin{pmatrix} e(k) & 0 \\ 0 & o(k) \end{pmatrix} .$$

As we can see, the off-diagonal elements are zero, i.e., there is no mode-mixing: if the configuration of incoming waves is even, the output state cannot be odd and vice versa. Inspecting the S-matrix at a wavenumber k_0 corresponding to the time-reversed state of an, e.g., even pole, the S-matrix will become

$$\widetilde{S}(k_0) = \begin{pmatrix} e(k_0) & 0 \\ 0 & o(k_0) \end{pmatrix} = \begin{pmatrix} 0 & 0 \\ 0 & \underbrace{o(k_0)}_{\neq 0} \end{pmatrix} .$$

Therefore, multiplying with the even eigenvector $(1,0)^T$ will produce no outgoing wave. Nevertheless, if we were to send an odd incoming wave, e.g, $(0,1)^T$, onto the system at wavenumber k_0, there would be *non-zero* scattering; zeros are only 'active' for a specific eigenstate of the S-matrix (the same goes for poles). This principle was, for example, applied for the experimental realisation of coherent perfect absorption in a random medium [3], where a waveguide system is furnished with loss in such a way that the a zero moves onto the real axis. At the corresponding frequency the system swallows the incoming eigenstate without any back-reflection.

As we have demonstrated, poles and zeros have designated eigenstates. But what about the non-diagonal description that we typically use for S-matrices? Using the eigenvalues $e(k)$ and $o(k)$ to represent (3.4) we get

$$S(k) = \begin{pmatrix} r(k) & t(k) \\ t(k) & r(k) \end{pmatrix} = \frac{1}{2} \begin{pmatrix} e(k) - o(k) & e(k) + o(k) \\ e(k) + o(k) & e(k) - o(k) \end{pmatrix} .$$

From the previous considerations it is clear that 'steering' the system into a pole, no matter if even or odd, gives infinities in all entries, while steering the system

[5] A function $f(z)$ is even if $f(-z) = f(z)$ and odd if $f(-z) = -f(z)$.

into a zero might not give a zero-entry at all. Therefore, in the non-diagonal case, the position of the zeros is generally unknown. It is even conceivable that certain poles cannot appear in certain entries. This fact poses a severe limitation for the method presented in [33], which we will briefly discuss in Section 4.2.2.

Chapter 4.

Quasi-Normal Mode Expansion of the Scattering Matrix

In this chapter we have a look at several approaches to formulating a semi-analytical expression for the S-matrix. By 'semi-analytical' we mean an analytical series expansion which depends on numerically calculated coefficients that, in turn, depend on the QNMs, i.e., their complex wavenumbers or frequencies and (far-)fields.

Having such a semi-analytical form has decisive advantages: for one, it allows to evaluate the S-matrix at arbitrary points[1]. Conventional (numerical) methods for calculating the S-matrix need to be re-run for every discrete frequency point which can take a considerable amount of time, as will be reported later. For the semi-analytical expression, however, we need to run similar routines only to solve for the dominant QNMs inside the desired frequency interval, leading to—potentially huge—speed-ups in computation. Moreover, while numerical routines can be considered as black-boxes that spit out numbers, a QNM-expansion allows for a transparent description and a better understanding of complex scattering systems based on which, e.g., resonant nanostructures can be optimised [33].

First, we examine Alpeggiani's work [34] and show that his formalism fails to deliver meaningful results for our complex waveguide structure: the reconstructed spectrum differs wildly from the reference and violates unitarity, a property that should be fulfilled as there is no absorption or gain in the system.

This observation led Salihbegović to modify Alpeggiani's derivation in order to enforce unitarity [35]. Naturally, the resulting S-matrix is unitary, nevertheless, it loses its transposition symmetry and thus violates reciprocity (which can be seen as an even more fundamental property in our case). Surprisingly, the total transmissions are reconstructed accurately.

Lastly, we present Weiss' method [36] for the one-dimensional Fabry-Pérot (1DFP). In contrast to the previously mentioned approaches, its derivation appears to be more sound and all in all more promising. The implementation,

[1] Of course, the series has to be truncated at some point, meaning that the expansion is only valid in a certain range that is determined by the set of selected QNMs.

however, has to overcome some obstacles which render this approach not quite as convenient as the others.

4.1. Alpeggiani's Approach

4.1.1. Derivation

In a 2017 PRX article [34], Alpeggiani and his coauthors presented a derivation of a semi-analytical formula for the S-matrix which will be summarised here.

Alpeggiani starts with a coupled mode ansatz: incoming waves in the channel basis, denoted $\mathbf{s}_+$, couple to modes $\mathbf{a}$ which consecutively couple to outgoing waves $\mathbf{s}_-$. The time evolution of the modes in the absence of any incoming wave is governed by some Hamiltonian H

$$\frac{\mathrm{d}\mathbf{a}}{\mathrm{d}t} = iH\mathbf{a}\,. \tag{4.1}$$

For the stationary case with time dependence $\exp(i\omega t)$ of $\mathbf{a}$, (4.1) is solved by the matrix exponential $\mathbf{a} = \mathbf{a}_0 \exp(iHt)$. In order to describe the coupling to QNMs, Alpeggiani chooses H in such a way that its eigenstates are exactly the QNMs, $\mathbf{a}_m$, with complex eigenfrequencies ω_m (or eigenenergies in the quantum mechanical context). Let us denote this Hamiltonian as H_{QNM} for which the eigenequation is

$$H_{\mathrm{QNM}}\mathbf{a}_m = \omega_m \mathbf{a}_m\,. \tag{4.2}$$

It must be mentioned that, although the authors call H_{QNM} the *effective Hamiltonian*, it is not the same as what *we* call the effective Hamiltonian, H_{eff}, that is derived in Appendix A: On one hand, H_{QNM} is energy-*independent* and has solely the QNMs as its eigenstates. On the other hand, H_{eff} is energy-*dependent* and its eigenstates are the so-called Constant Flux states (CF states) [30]. Due to its skew-Hermitian property, these CF states form a biorthogonal basis [37]. Now, Alpeggiani assumes that the 'artificial' Hamiltonian H_{QNM} always exists and is skew-Hermitian, i.e., it has a biorthogonal basis with the right-eigenstates being the QNMs. Following these assumptions and the fact that QNMs have complex frequencies, we can write $H_{\mathrm{QNM}} = \Omega + i\Gamma$, where Ω and Γ are both Hermitian.

Plugging H_{QNM} into (4.1), introducing coupling between the modes and the incoming waves through $K^T\mathbf{s}_+$, as well as introducing the equation for outgoing waves via the out-coupling of the modes and the direct coupling of incoming waves, we arrive at the coupled mode equations:

$$\begin{aligned} i\omega\mathbf{a} &= i\left(\Omega + i\Gamma\right)\mathbf{a} + K^T\mathbf{s}_+\,, \\ \mathbf{s}_- &= C\mathbf{s}_+ + D\mathbf{a}\,. \end{aligned} \tag{4.3}$$

Due to physical reasons there exist some useful relations between the coupling matrices K and D, the direct coupling matrix C and Γ [38], namely

$$K = D\,, \tag{4.4}$$
$$\Gamma = \frac{1}{2} D^\dagger D\,,$$
$$CD^* = -D\,. \tag{4.5}$$

The S-matrix connects outgoing to incoming waves, $\mathbf{s}_- = S\mathbf{s}_+$. By solving (4.3) for $\mathbf{s}_-$ and using Equations (4.4) and (4.5) we arrive at

$$S = C - iD(\omega\mathbb{1} - \Omega - i\Gamma)^{-1} D^T\,. \tag{4.6}$$

Next, Alpeggiani expands the S-matrix in such a way that it depends only on the complex frequencies ω_m and the far-fields of the QNMs. For this we define $A \coloneqq (\mathbf{a}_1, \mathbf{a}_2, ...)$ and write all of the eigenequations (4.2) compactly as[2]

$$(\Omega + i\Gamma)A = A\widetilde{\Omega}\,,$$

where $\widetilde{\Omega} = \mathrm{diag}(\omega_1, \omega_2, ...)$ is the diagonal matrix containing the complex eigenfrequencies. Due to the assumed biorthogonality, we do the same for the left-eigenvectors of H_{QNM}

$$L^\dagger(\Omega + i\Gamma) = L^\dagger\widetilde{\Omega}\,.$$

We can now expand $\omega\mathbb{1} - H_{\mathrm{QNM}}$ as

$$\omega\mathbb{1} - \Omega - i\Gamma = A\left(\omega\mathbb{1} - \widetilde{\Omega}\right)L^\dagger\,.$$

Substituting this expansion in (4.6) and using $L^\dagger = A^{-1}$ [37] yields[3]

$$\begin{aligned} S &= C - iD\left(A\left(\omega\mathbb{1} - \widetilde{\Omega}\right)L^\dagger\right)^{-1} D^T = \\ &= C - iDA\left(\omega\mathbb{1} - \widetilde{\Omega}\right)^{-1} A^{-1} D^T = \\ &= C - iDA\left(\omega\mathbb{1} - \widetilde{\Omega}\right)^{-1} A^{-1}\left((A^T)^{-1}A^T\right) D^T = \\ &= C - iDA\left(\omega\mathbb{1} - \widetilde{\Omega}\right)^{-1} \Lambda^{-1}(DA)^T\,, \end{aligned}$$

[2] Writing the eigenstate in front of the eigenvalue, i.e. $A\widetilde{\Omega}$, might seem strange at first, but is necessary when compacting all eigenequations in matrix notation.
[3] Keep in mind that $(AB)^{-1} = B^{-1}A^{-1}$ as well as $(AB)^T = B^T A^T$.

with the diagonal matrix $\Lambda \coloneqq A^T A$ [34].

The term DA collects all the far-fields of the QNMs: consider the case of only one QNM $\mathbf{a}_{m'}$ being active; by definition there are no incoming waves and thus the outgoing wave, i.e., the far-field, is simply the out-coupling of the QNMs described by D, cf. (4.3). We therefore define

$$\begin{aligned} \mathbf{b}_m &\coloneqq \mathbf{s}_-|_{\omega=\omega_m} = D\mathbf{a}_m \\ B &= (\mathbf{b}_1, \mathbf{b}_2, ...) = DA\,. \end{aligned}$$

The vectors b_m and thus the matrix B can be obtained by evaluating the QNM-field sufficiently far away from the scattering region in the channel basis. As is shown in [34], the normalisation can be chosen freely; only the relative complex amplitudes contained in the b_ms are important.

With the above, the S-matrix becomes

$$S = C - iB\left(\omega\mathbb{1} - \widetilde{\Omega}\right)^{-1}\Lambda^{-1}B^T\,.$$

In order to evaluate Λ, Equation (4.5) is extended [34] to read

$$CB^* + B\Lambda^{-1}Q^* = 0\,, \tag{4.7}$$

where $Q = A^\dagger A$. The entries of Q can be shown to be [34]

$$Q_{ij} = i\frac{\mathbf{b}_i^\dagger \mathbf{b}_j}{\omega_j - \omega_i^*}\,. \tag{4.8}$$

Equation (4.7) remains to be solved for Λ. However, the problem is over-determined since the dimensions of B are the number of channels, N, times the number of QNMs, M, and therefore $N \times M$, while the number of diagonal entries of Λ (which we need to solve for) is N. Hence, for given C, a solution is not guaranteed to exist. Alpeggiani mentions that C could be chosen to make (4.7) solvable for Λ but claims this would be increasingly difficult with a larger number of QNMs. Consequently, he considers C to be given—presumably from physical considerations—and continues to find an approximate solution in the least squares sense. The resulting diagonal entries of Λ^{-1} are

$$\frac{1}{\lambda_j} = -\frac{\sum_{mm'} Q^{-1}_{mj}(Q^{-1}_{m'j})^* \mathbf{b}_m^T C^\dagger C \mathbf{b}^*_{m'}}{\sum_m Q^{-1}_{mj}\mathbf{b}_m^T C^\dagger \mathbf{b}_j}\,,$$

leading to the final expression for the S-matrix

$$\boxed{S_{\text{alpe}} = C + i\sum_m \frac{1}{\lambda_m}\frac{\mathbf{b}_m \mathbf{b}_m^T}{\omega - \omega_m}}\,. \tag{4.9}$$

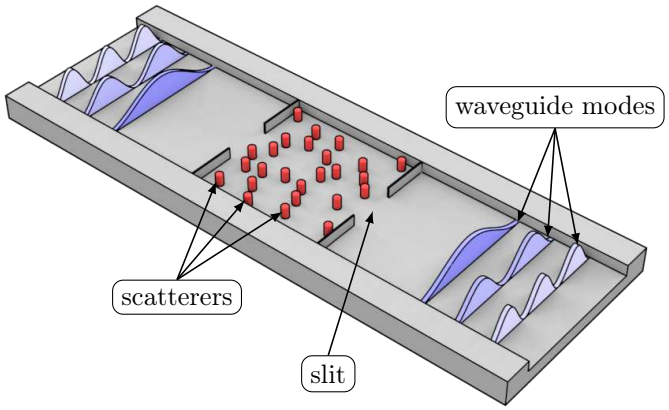

Figure 4.1.: 3D visualisation of the geometry and potential of the 2D system: a quadratic scattering region of side length $L = 4.35$ is embedded into an infinite two-dimensional waveguide. It is connected via two slits of length $L/3$. Between the slits are 25 randomly distributed scatterers (in red) with diameter $r = 0.025L$ and constant potential $V = 95.86E_0$, where $E_0 = \frac{1}{2}\left(\frac{\pi}{L}\right)^2$. The blue waves indicate the first three waveguide modes on either side. We will consider an energy interval which will allow up to eight open modes per port.

only depends on the complex eigenfrequencies ω_m, the far-fields of the according QNMs and the direct coupling matrix C which, however, is chosen to be the identity, $C = \mathbb{1}$, in all examples presented in [34].

4.1.2. A Complex 2D Waveguide

In order to test Alpeggiani's expansion we devised a complex scattering geometry similar to structures already studied in numerous publications [1, 3, 12, 16]. Note, that we set off to solve the Schrödinger Equation (SE) instead of Maxwell's equations or the Helmholtz equation[4].

As shown in Figure 4.1, we started from a rectangular two-dimensional infinite waveguide, in which we randomly placed 25 scatterers inside a quadratic region. These circular scatterers have constant potential. Inside the waveguide the po-

[4]For many problems the Helmholtz equation describes the physics sufficiently, avoiding the need to solve the full set of Maxwell's equations. Furthermore, the Schrödinger and the Helmholtz equation are, at least for our use-cases, equivalent [39]. So in a very limited sense it does not matter which of the three equations is employed.

tential is zero and infinite at the boundaries or 'walls'. Also, we enclosed the scattering region by two additional walls, each with a slit, to increase the decay time[5] of the modes, leading to a more pronounced resonance spectrum. This measure prevents very broad resonances to occur which would be hard to incorporate into our calculation. We are interested in the S-matrix over an energy interval that allows up to eight open waveguide modes per side. Consequently, we need to calculate an S-matrix of dimension 16×16. In order to verify whether or not the QNM-expansion works, we expressed the reference S-matrix via the effective Hamiltonian formula $S = \mathbb{1} - iW^\dagger G_{\text{eff}} W$ (Appendix A) and computed the effective Green's function through a recursive Green's function approach [18].

In order to use Equation (4.9), we require the QNM far-fields and their complex energies. Unfortunately, for our waveguide structure it is not clear how to reliably calculate these quantities (see [26] for an overview). In the end, we opted for a Perfectly Matched Layer (PML) approach. For the details we refer to [35]. However, it shall be noted that PMLs introduce a considerable amount of *numerical QNMs*, i.e., unphysical QNMs, that have to be filtered out: most of them automatically, some of them, however, manually, due to the lack of robust filtering criteria. For the remainder of this work, we will not worry about such problems and take the QNMs as given or derive them analytically. Nonetheless, making the QNM-expansion work for 'practical' purposes requires an efficient QNM-solver which, in general, poses a non-trivial problem.

4.1.3. Results for the Complex 2D Waveguide

Using Alpeggiani's method on the complex 2D-waveguide presented in the previous section leads to a strongly non-unitary S-matrix, as can be seen from the total transmissions and reflections plotted in Figure 4.2. This glaring discrepancy led Salihbegović to propose a unitarity correction to Alpeggiani's approach with which the total transmissions and reflections are reconstructed accurately as we will show in the next section.

[5] Think of the wave as a particle which bounces back and forth inside the scattering region. Since the only way it can leave is through the slits, it will take more time to escape if the slits are narrower.

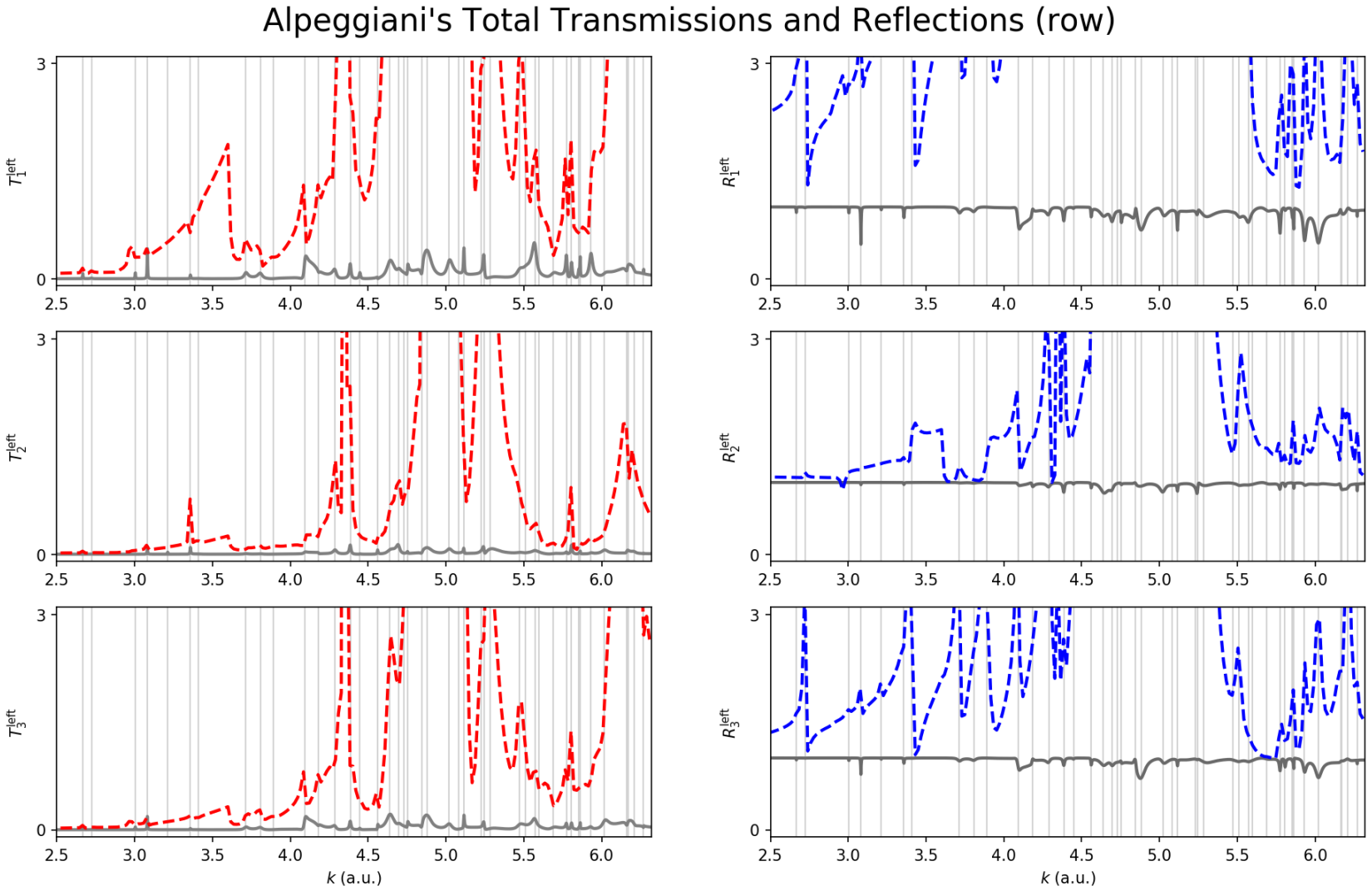

Figure 4.2.: Total transmissions (red) and reflections (blue) (sum over row entries) reconstructed via Alpeggiani's approach versus our numerical reference (grey). Vertical lines mark the positions of the QNMs. Obviously, Alpeggiani's reconstruction does not yield meaningful results, as it neither matches the reference nor conforms to unitarity with peaks well above unity.

4.2. Salihbegović's Approach: a Unitarity Correction

As seen in the previous section, Alpeggiani's approach applied on our complex waveguide structure leads to a strongly non-unitary S-matrix. In Salihbegović's master-thesis [35], one possible explanation is pointed out: under certain assumptions (see below) Alpeggiani's S-matrix turns out to be non-unitary for complex-valued far-field coefficients $\mathbf{b}_m$. Real-valued far-field coefficients, though, can only be found for highly symmetric problems. Our waveguide does not fall under this category as there is no inherent symmetry.

We repeat Salihbegović's argument here: inserting Alpeggiani's formula (4.9) into the defining equation of unitarity for the S-matrix, $SS^\dagger = \mathbb{1}$, yields

$$\left(C + i\sum_m \frac{1}{\lambda_m}\frac{\mathbf{b}_m\mathbf{b}_m^T}{\omega-\omega_m}\right)^\dagger \left(C + i\sum_m \frac{1}{\lambda_m}\frac{\mathbf{b}_m\mathbf{b}_m^T}{\omega-\omega_m}\right) = \mathbb{1}\,. \tag{4.10}$$

If we now assume $C = \mathbb{1}$, as is done for all examples presented in [34], and furthermore assume that the system has only one QNM[6], (4.10) becomes

$$\frac{i}{\lambda_1^*}\frac{\left(\mathbf{b}_1\mathbf{b}_1^T\right)^\dagger}{\omega-\omega_1^*} - \frac{i}{\lambda_1}\frac{\mathbf{b}_1\mathbf{b}_1^T}{\omega-\omega_1} + \frac{1}{\lambda_1\lambda_1^*}\frac{\left(\mathbf{b}_1\mathbf{b}_1^T\right)^\dagger\mathbf{b}_1\mathbf{b}_1^T}{(\omega-\omega_1)(\omega-\omega_1^*)} = \mathbb{0}\,. \tag{4.11}$$

Noting that

$$\left(\mathbf{b}_1\mathbf{b}_1^T\right)^\dagger\mathbf{b}_1\mathbf{b}_1^T = \mathbf{b}_1^*\underbrace{\mathbf{b}_1^\dagger\mathbf{b}_1}_{=\text{scalar}}\mathbf{b}_1^T = \mathbf{b}_1^\dagger\mathbf{b}_1\;\mathbf{b}_1^*\mathbf{b}_1^T\,,$$

we cast (4.11) into a sum of three matrices, each multiplied by some scalar (for fixed ω):

$$f_1(\omega)\left(\mathbf{b}_1\mathbf{b}_1^T\right)^\dagger + f_2(\omega)\mathbf{b}_1\mathbf{b}_1^T + f_3(\omega)\mathbf{b}_1^*\mathbf{b}_1^T = \mathbb{0}\,, \tag{4.12}$$

which has to hold for all ω and $f_i(\omega) \neq 0$. Therefore, $\left(\mathbf{b}_1\mathbf{b}_1^T\right)^\dagger$, $\mathbf{b}_1\mathbf{b}_1^T$ and $\mathbf{b}_1^*\mathbf{b}_1^T$ have to be linearly dependent. Otherwise, (4.12) cannot hold except for the trivial case. Here, linear dependence equates to the three matrices differing only by some complex factor. While this is true for *real-valued* $\mathbf{b}_m$, it is not for complex-valued

[6] This assumption is justified as follows: even though we expect the number of QNMs to be infinite for any system, it is not far-fetched to devise an example where only one QNM is crucial for the description of the scattering process; at least over some restricted spectral range. If a formalism cannot even yield a unitary S-matrix for this simple case (as Salihbegović shows for Alpeggiani's approach) it would be surprising if it did when including several modes.

$\mathbf{b}_m$ as can be easily checked. However, as stated earlier, non-symmetric systems will in general feature *complex-valued* $\mathbf{b}_m$.

Curiously, by exchanging the transpose with a complex transpose in (4.9) ($B^T \to B^\dagger$) and flipping the sign modifies Alpeggiani's expansion to be unitary in general. Furthermore, the Λ-matrix, $\Lambda = AA^T$, becomes $AA^\dagger$ which is the Q-matrix given in Equation (4.8). This renders the least squares fit, described in Section 4.1.1, superfluous. The unitarity-corrected Alpeggiani expansion is thus:

$$\boxed{S_{\text{uc}} = \mathbb{1} + iB(\mathbb{1}\omega - \widetilde{\Omega})^{-1}Q^{-1}B^\dagger}. \tag{4.13}$$

4.2.1. Results for the Complex 2D Waveguide

Again, we tested the unitarity-corrected version of Alpeggiani's expansion on our complex waveguide problem described in Section 4.1.2. As expected, our S-matrix is strictly unitary. The reconstructed total row transmissions and reflections, i.e., the sum over a row of entries of the corresponding submatrix, $\sum_j T_{ij}^{\text{left/right}}$ and $\sum_j R_{ij}^{\text{left/right}}$, match the reference very well; see Figure 4.3. The peak around $k \approx 4.1$([7]) presents a conspicuous exception to the otherwise faithful reconstruction. It is most likely that the corresponding QNM was either not found or filtered out accidentally. As reported in [35], computing the reference S-matrix at 3000 energy points took about 11 hours on the Vienna Scientific Cluster (using 16 nodes) while calculating the raw QNM-data merely took around 40 minutes on the same system. The filtering and reconstruction (for the same 3000 energy points) was done on a single-CPU system and required an additional hour or so[8]. This demonstrates the enormous speed-up potential.

Nevertheless, the resulting S-matrix is not transposition-symmetric and thus violates reciprocity. As a consequence, the single entries $T_{ij}^{\text{left/right}}$ of the two transmission submatrices differ and indeed both of them do not match the transposition-symmetric reference, see Figure 4.4. Sums over columns are incorrect as well, as can be seen in Figure 4.5.

[7] The exact units are arbitrary for our purposes and thus omitted altogether.

[8] Again, the filtering process required human intervention and was thus run on an office PC. Without these issues, filtering could be done efficiently on the cluster; presumably adding only a negligible amount of computation time.

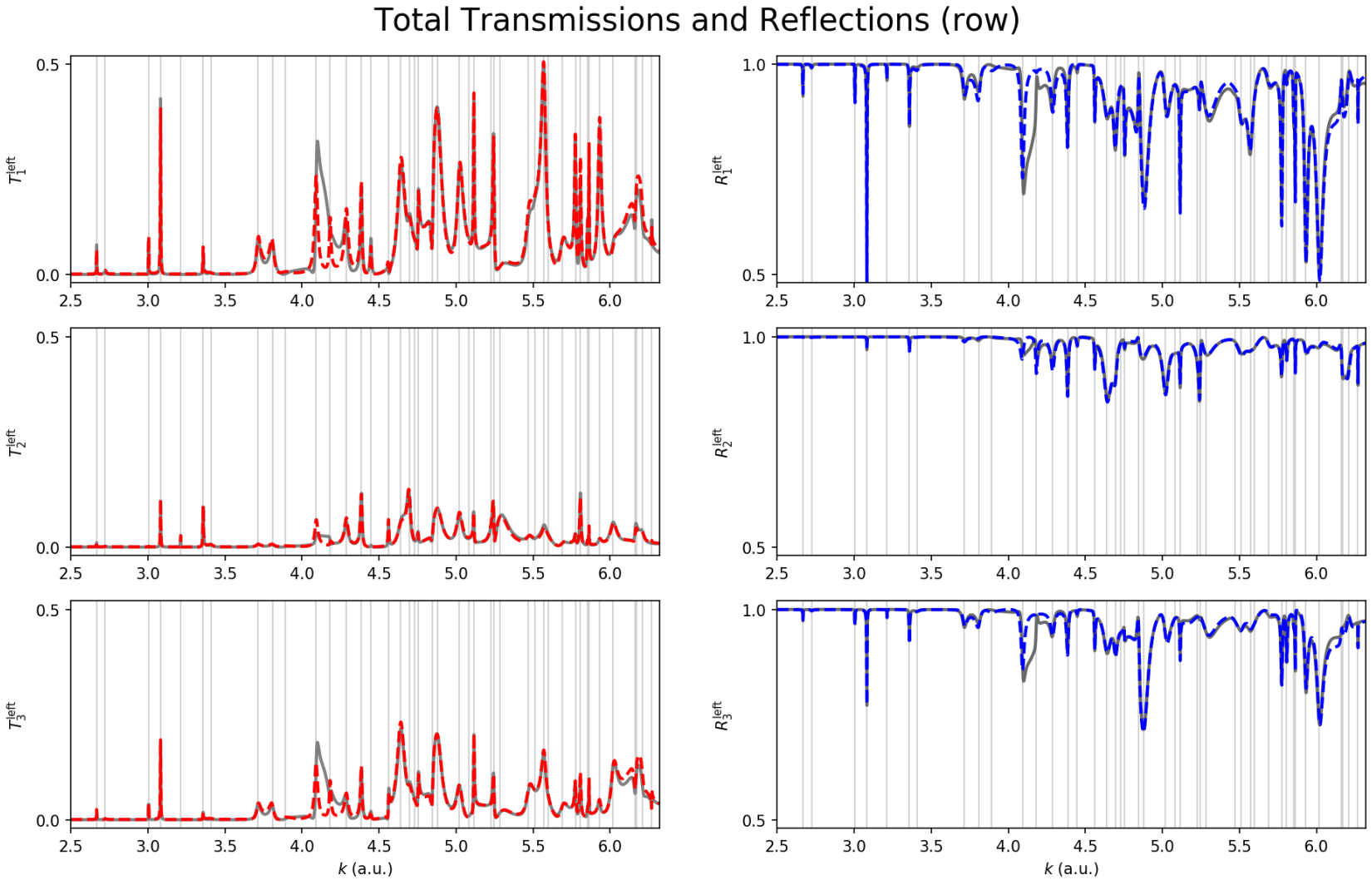

Figure 4.3.: Total transmissions $T^{\text{left}}_{i,} = \sum_j T^{\text{left}}_{ij}$ (red) and reflections $R^{\text{left}}_{i,} = \sum_j R^{\text{left}}_{ij}$ (blue) of the first three rows vs. the corresponding references (grey). Vertical lines mark the positions of the QNMs. Disregarding the peak at $k \approx 4.1$, the reconstruction is accurate.

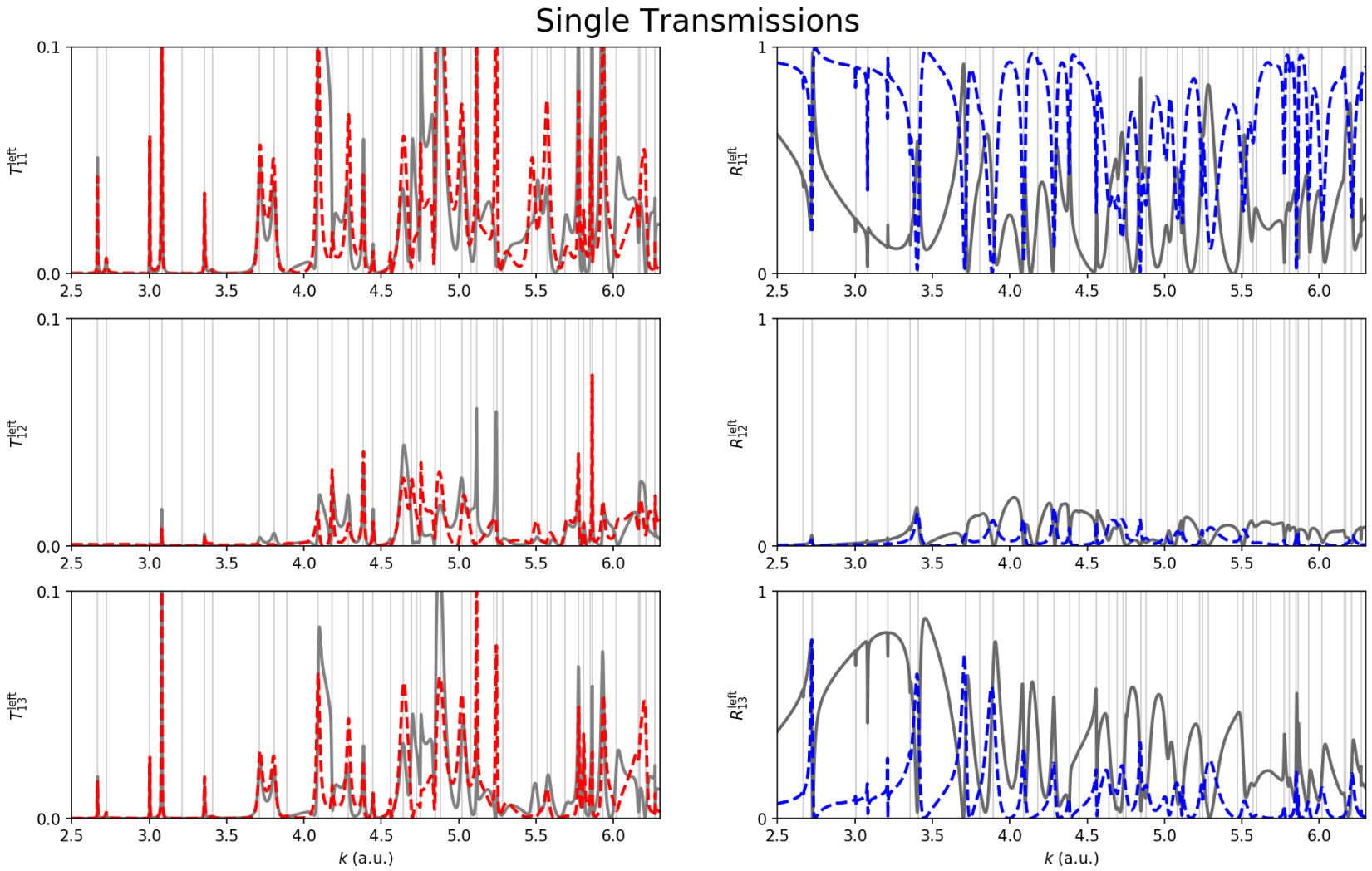

Figure 4.4.: First three erroneous single transmissions T_{1i}^{left} (red) and reflections R_{1i}^{left} (blue) versus the reference (grey) of the first row. Vertical lines mark the positions of the QNMs. While each single entry does not match the reference, their sum, including the five transmissions and reflections of the same row which are not shown here, surprisingly reconstructs the total transmission or reflection accurately, see the top plots of Figure 4.3.

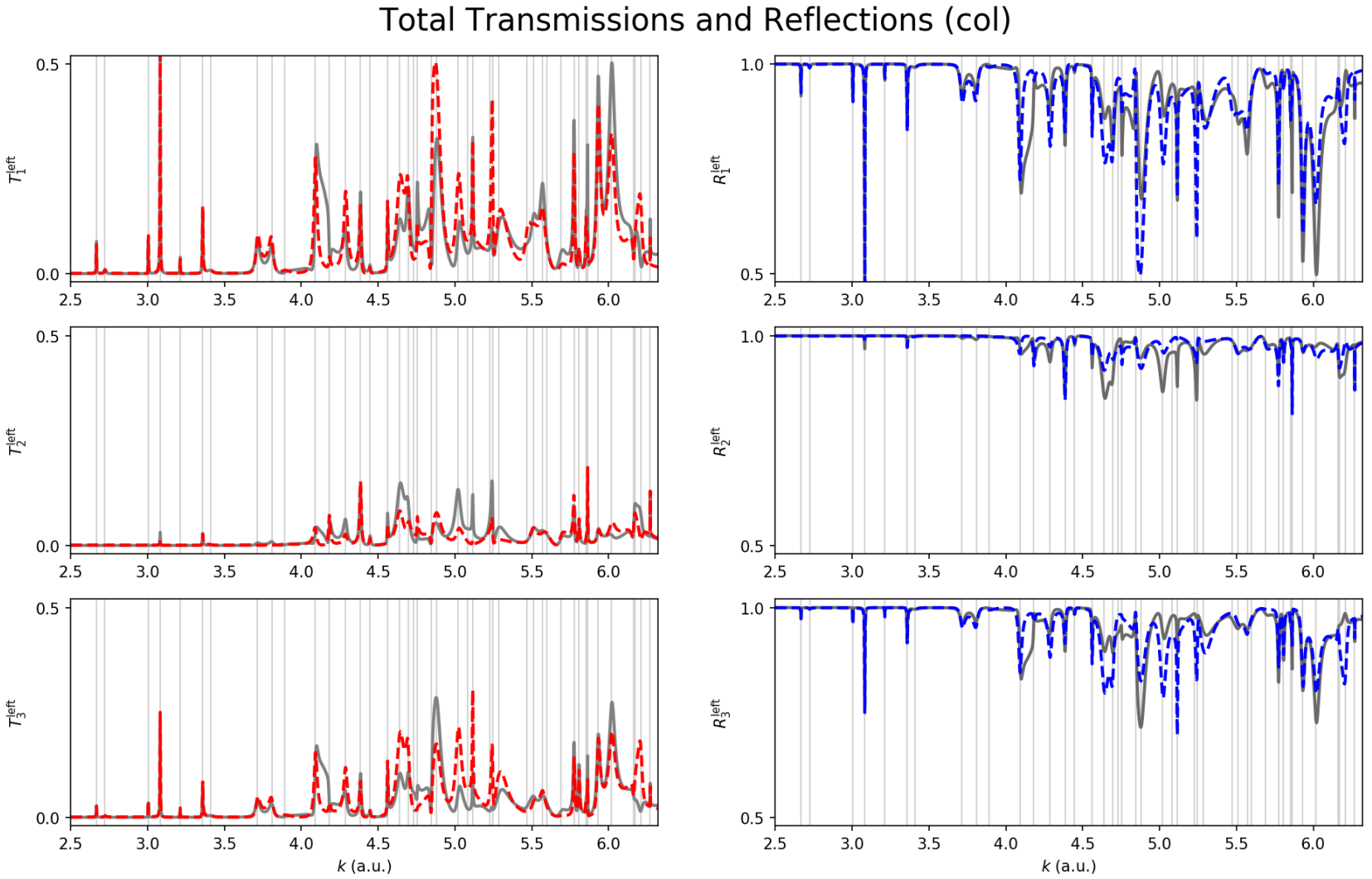

Figure 4.5.: Erroneous total transmissions $T^{\text{left}}_{,j} = \sum_i T^{\text{left}}_{ij}$ (red) and reflections $R^{\text{left}}_{,j} = \sum_i R^{\text{left}}_{ij}$ (blue) versus the reference (grey) of the first three columns. Vertical lines mark the positions of the QNMs. Opposed to the total row transmissions and reflections, which get reconstructed correctly, the total column transmission and reflections, shown here, do not match the reference.

4.2.2. Correcting the Correction

It is astonishing how Salihbegović's unitarity constraint amends Alpeggiani's approach, transforming its flawed results into solid reconstructions for the total scattering quantities. What exactly our expansion is missing and why it works the way it does remains unresolved, though. In an effort to correct these shortcomings we tackled the problem from different angles which, albeit unsuccessful, are documented here.

We started out seeking a possibly missing 'background term', S_{bg}, which would correct the single entries and restore the transposition symmetry of S_{uc} (Equation (4.13)). We based our search on an ansatz that combines the Dyson equation $G = G_0 + G_0 \Delta V G$ with the effective Hamiltonian expression for the S-matrix, Equation (2.8):

$$S = \mathbb{1} - iW^\dagger G_{\mathrm{eff}} W = \mathbb{1} - iW^\dagger G_{\mathrm{eff},0} W - iW^\dagger G_{\mathrm{eff},0} \Delta V G_{\mathrm{eff}} W \,.$$

From the comparison

$$S = S_{\mathrm{bg}} + S_{\mathrm{uc}} \longleftrightarrow S = \mathbb{1} - \underbrace{iW^\dagger G_{\mathrm{eff},0} W}_{=:S_{\mathrm{bg}}} - iW^\dagger G_{\mathrm{eff},0} \Delta V G_{\mathrm{eff}} W \,,$$

we need to find $G_{\mathrm{eff},0}$ or, equivalently, a perturbation term ΔV (which would allow us to calculate $G_{\mathrm{eff},0}$). The ansatz is universal and one can always construct such an S_{bg}. However, we hoped to find a physically meaningful background this way: by interpreting the Dyson equation, S_{bg} would describe a scattering system on its own, that, perturbed by some ΔV, would yield the whole system described by S. Unfortunately, we could not make this ansatz work.

While tinkering with this idea we invested some effort into better understanding the effective Hamiltonian formalism that led to the derivation presented in Appendix A. In essence, the formalism is based on Feshbach's projection operator formalism that separates the Schrödinger equation into two coupled equations, one of which is defined on the so-called Q-space while the other is defined on the so-called P-space. The Q-space is the 'inner' space containing the scattering region while the P-space is the 'outer' space containing the asymptotic region[9]. Solving the coupled equations subject to an incoming wave in P-space eventually leads to the expression $S = \mathbb{1} - iW^\dagger G_{\mathrm{eff}} W$, where W represents the coupling between P- and Q-space and G_{eff} describes the propagation of the incoming wave in Q-space. In a work by Domcke [40], Feshbach's theory is extended, such that an explicit background term arises as a consequence of *orthogonality scattering*, which occurs if the Q- and P-space bases are not chosen orthogonally. Using the fact that

[9] It shall be noted that the partition into P- and Q-space is arbitrary and does not necessarily need to divide coordinate-space. However, this choice is most convenient for our use-case since outside the scattering region there is only free space propagation.

QNMs are complete inside the scattering region[10] [19, 41], we explored the idea of choosing the QNMs as the Q-space basis states in the hope that we could either fix our approach by integrating Domcke's background term or find another (working) QNM expansion altogether. Neither could be achieved, although we cannot rule out that our implementation failed to handle the technical and mathematical details correctly (for example the complicated completeness relation for the QNMs, cf. Equation (C.6)). We still think that the combination of QNMs and Domcke's theory (or more generally Feshbach's theory) is worth pursuing, especially since Weiss noted that parts of his formalism for expanding the S-matrix—which will be presented in the next section—could be derived in a more elegant manner within this framework.

Another approach was to correct our S-matrix by finding a general pattern in the error terms, see Figure 4.6. With the ansatz $T_{\mathrm{uc},ij}^{\mathrm{left/right}} = T_{ij}^{\mathrm{left/right}} + \Delta T_{ij}^{\mathrm{left/right}}$, where $T_{\mathrm{uc}}^{\mathrm{left/right}}$ is our erroneous (left or right) transmission submatrix, $T^{\mathrm{left/right}}$ is the correct reference submatrix and $\Delta T^{\mathrm{left/right}}$ contains the respective error terms. In order to calculate all of the $2n^2$ error terms $\Delta T_{ij}^{\mathrm{left/right}}$, where n is the number of open channels per side, we would need $2n^2$ linear and independent equations. If we assume that our total transmissions are correct and demand transposition symmetry we arrive at

$$\begin{aligned} \sum_j \Delta T_{ij}^{\mathrm{left}} &= 0, \quad \forall i \\ \sum_j \Delta T_{ij}^{\mathrm{right}} &= 0, \quad \forall i \\ \Delta T_{ij}^{\mathrm{left}} &= \Delta T_{ji}^{\mathrm{right}}, \quad \forall i, j\,, \end{aligned}$$

amounting to $2n + n^2$ equations, i.e., too few. With a little bit of imagination, however, we can spawn $n/2$ additional equations for each equation counted in the $2n$ term: inspecting Figure 4.6 reveals that neighbouring error terms (e.g. light and dark orange) sum to zero. Of course, this poses a very crude approximation but if it were true we could extend our previous set of equations by the pairing equations $\Delta T_{i(j+1)}^{\mathrm{left/right}} = -\Delta T_{ij}^{\mathrm{left/right}}$, yielding the required $2n^2$ equations of which, unfortunately, only $2n^2 - 2n$ are linearly independent. Similar attempts to define a correcting unitarity transform also failed due to too many degrees of freedom.

[10] Otherwise, there would be an additional background term capturing non-trivial scattering (meaning other than free-space propagation) in P-space.

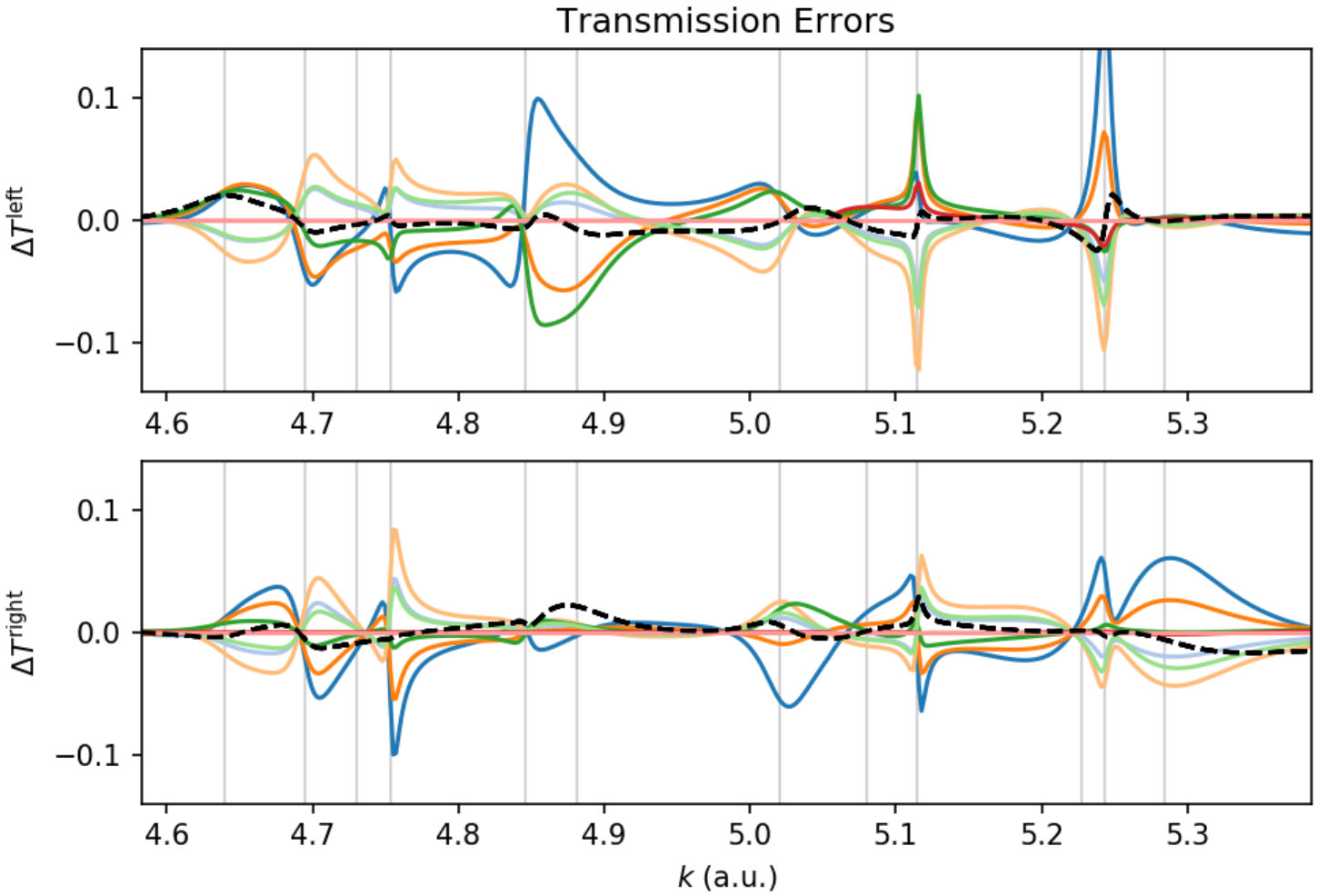

Figure 4.6.: Error terms ΔT^{left} (top) and ΔT^{right} (bottom) in solid lines for the respective first rows over a restricted section of the spectrum. The dashed line is the total error which we treated as sufficiently flat and close to zero. Vertical lines mark the positions of the QNMs.

Yet another approach was inspired by publications of Grigoriev [33] and Colom [42]: any meromorphic function can be expanded through a Weierstrass factorisation, an infinite product over pole terms. By converting this product into a sum via partial fractions, one obtains[11]

$$f(z) = A\exp(iBz)\left(1 + \sum_m \frac{r_m}{z - p_m}\right),$$

with

$$A = f(0)\prod_m \frac{p_m}{q_m},$$
$$iB = \frac{\frac{\mathrm{d}f}{\mathrm{d}z}\big|_{z=0}}{f(0)} + \sum_m \left(\frac{1}{q_m} - \frac{1}{p_m}\right),$$
$$r_m = (p_m - q_m)\prod_{n\neq m} \frac{p_m - q_n}{p_m - p_n},$$

where p_m is the m^{th} pole, q_m is the m^{th} zero and r_m is the corresponding residue (originating from the partial fraction expansion). Also note that we could employ the symmetry relations of the QNMs $p_{-m} = -p_m^* \Rightarrow r_{-m} = -r_m^*$ and $q_m = -p_m$ (time-reversal symmetry) to further simplify the expressions. Since we can incorporate only some finite number M of poles, i.e., QNMs, there will be a truncation error for which Colom derives a compensation term [42]. After introducing aforementioned term into Grigoriev's expansion we get

$$f(z) = A\exp(iBz)\left(1 + \sum_{m=-M}^{M} \frac{r_m}{p_m} + \sum_{m=-M}^{M} + \frac{r_m}{z - p_m}\right). \tag{4.14}$$

In [33], a diagonal S-matrix is assumed[12] and consequently each diagonal entry is expanded in the form (4.14). However, this method is limited. Firstly, it might not be obvious which poles and zeros of the system have to be assigned to what diagonal element. Secondly, when considering non-diagonal S-matrices and their off-diagonal elements the corresponding zeros will be unknown (see Chapter 2). Furthermore, entries that go to zero as $\omega \to 0$ would need to be expanded around another point because in that case $A = 0 \Rightarrow f(z) = 0$. Remarkably, Salihbegović's form (4.13) is equivalent to (4.14) for scattering systems with only one channel[13], disregarding the factor $A\exp(iBz)$, which might, however, be inherently contained in the far-field information and is arbitrary for this sort of simple system.

[11] See the supplemental material of [33] for a concise and beautiful derivation.

[12] This assumption is easily justified for spherically symmetric systems represented in a multi-pole basis.

[13] With only one channel there can only be reflection. Consequently, the S-matrix becomes a 'scattering scalar', i.e., a complex phase of the form $e^{i\theta(k)}$ (for unitary systems).

4.3. Weiss' Approach

The last approach we pursued yields the most promising results. It is rooted in the Resonant State Expansion (RSE)—a perturbation theory for QNMs—which has been successfully demonstrated and extended in numerous publications [25, 43, 44, 45, 46, 47, 48]. It employs the analytical normalisation of QNMs [24, 25] to express the Green's function via the Mittag-Leffler (ML) expansion. Based on this, an expression for the ML-expansion of the S-matrix is derived by Weiss [36]. Weiss' derivation appears to be more solid when compared to Alpeggiani's method and yields very good results as is shown in detail for a simple one-dimensional example in Section 4.3.5. However, in its current form it still requires the complete information of the wave inside the scatterer in order to normalise the QNMs. So in contrast to Alpeggiani's approach, knowing just the far-fields of the QNMs does not suffice. In the case of periodic structures, the QNMs can be computed via the Fourier modal method in such a way that the resulting QNMs are already normalised [49]. Unfortunately, we are not aware of a similarly convenient method for computing the normalised QNMs for our complex waveguides.

Weiss formulates his S-matrix for Maxwell's equations quite generally [25, 36]. We will work with a more specific formulation that is especially suited for the Helmholtz Equation (HE) and is equivalent to the 'old' definitions found in earlier publications, e.g. [24]. Furthermore, we will restrict this discussion to one- and two-dimensional systems.

4.3.1. Basis States and Orthonormality

First, we present the orthonormality relations that must hold for the incoming, $\mathbb{I}_N$, and outgoing, $\mathbb{O}_N$, basis states which can otherwise be defined arbitrarily. These states will be used to expand the prescribed incoming wave as well as the scattered waves outside the scattering region that are generated by the aforementioned incoming wave. Inspired by Lorentz-reciprocity (cf. [13] Equation (6)) Weiss defines the following operations

$$[\phi(\mathbf{r})|\psi(\mathbf{r})]_{\partial\mathcal{V}} = \int_{\partial\mathcal{V}} \phi(\mathbf{r})\partial_s\psi(\mathbf{r}) - \psi(\mathbf{r})\partial_s\phi(\mathbf{r})\mathrm{d}S\,,$$
$$\langle\phi(\mathbf{r})|\psi(\mathbf{r})\rangle_{\mathcal{V}} = \int_{\mathcal{V}} \phi(\mathbf{r})\psi(\mathbf{r})\mathrm{d}V\,,$$

where the integral $\int_{\partial\mathcal{V}} \ldots \mathrm{d}S$ is taken along the surface of the minimal volume $\mathcal{V}$ enclosing the scattering region and ∂_s denotes the derivative along the surface's normal. With the above, Weiss specifies the orthonormality relations of the in-

coming and outgoing basis states:

$$[\mathbb{I}_N|\mathbb{I}_{N'}]_{\partial\mathcal{V}} = [\mathbb{O}_N|\mathbb{O}_{N'}]_{\partial\mathcal{V}} = 0\,, \tag{4.15}$$
$$[\mathbb{I}_N|\mathbb{O}_{N'}]_{\partial\mathcal{V}} = -\,[\mathbb{O}_{N'}|\mathbb{I}_N]_{\partial\mathcal{V}} = \delta_{NN'}\,. \tag{4.16}$$

To better illustrate these relations let us give an example: In the one-dimensional case we could choose $\mathbb{I}(z;k) = \sqrt{\frac{1}{2ik}}\exp(ikz)$ and $\mathbb{O}(z;k) = \sqrt{\frac{1}{2ik}}\exp(-ikz)$. The 'surface' (i.e. a point) is located at $z = 0$ and its normal is oriented in the $-z$-direction. One easily verifies that Equations (4.15) and (4.16) hold in this case. Note the difference to the typical orthonormality relation in quantum mechanics: $\langle\mathbb{I}_N|\mathbb{I}_N\rangle = 1 \longleftrightarrow [\mathbb{I}_N|\mathbb{O}_N]_{\partial V} = 1$. Also keep in mind that, while $\langle\cdot|\cdot\rangle$ is an integral over all of space, the operation $[\cdot|\cdot]_{\partial V}$ integrates only along the surface of the scattering region. Moreover, the basis states are defined exclusively on the outside plus the given surface. Their coupling to the inside is determined by surface terms of the form $\left[\mathbb{O}_N|\widetilde{\mathbb{F}}\right]_{\partial\mathcal{V}}$ where $\widetilde{\mathbb{F}}$ is the field inside the scattering region. In terms of the Feshbach projection operator formalism (see Appendix A), we would say that $\mathbb{I}_N$ and $\mathbb{O}_N$ are defined in P-space, and that the scattering in Q-space originates from the surface source terms $H_{QP}\,|\mathbb{I}_N\rangle$ (H_{QP} constitutes the 'surface').

Next, we expand the total field in the exterior as

$$\mathbb{F}(\mathbf{r};k) = \sum_N \alpha_N^{\text{in}}(k)\mathbb{I}_N(\mathbf{r};k) + \alpha_N^{\text{out}}(k)\mathbb{O}_N(\mathbf{r};k)\,,$$

where the expansion coefficients are defined by employing the orthonormality relations

$$\begin{aligned}\alpha_N^{\text{in}}(k) &= [\mathbb{O}_N|\mathbb{F}]_{\partial V}\ ,\\ \alpha_N^{\text{out}}(k) &= [\mathbb{I}_N|\mathbb{F}]_{\partial V}\ .\end{aligned} \tag{4.17}$$

It is easiest to choose the basis states $\mathbb{I}_N$ and $\mathbb{O}_N$ so that they coincide with the states of the channel basis, e.g, our waveguide modes, for which we seek to calculate the S-matrix; then

$$\begin{pmatrix}\alpha_1^{\text{out}}(k)\\ \alpha_2^{\text{out}}(k)\\ \vdots\end{pmatrix} = S(k)\begin{pmatrix}\alpha_1^{\text{in}}(k)\\ \alpha_2^{\text{in}}(k)\\ \vdots\end{pmatrix}\ .$$

In the following we usually 'activate' a single incoming channel, i.e., $\alpha_M^{\text{in}}(k) = 1$ and $\alpha_N^{\text{in}}(k) = 0\ \forall N \neq M$ which simplifies the calculations; for instance $\alpha_N^{\text{out}}(k) = S_{NM}(k)\alpha_M^{\text{in}}(k)$. The general case, $\alpha_N^{\text{out}}(k) = \sum_M S_{NM}(k)\alpha_M^{\text{in}}(k)$, is handled by means of linearity.

4.3.2. Mittag-Leffler Expansion

According to the Mittag-Leffler (ML) theorem [50], there always exists a meromorphic function for a set of prescribed poles and residues, that exhibits said poles and is determined by the corresponding residue in their vicinity. Indeed, such an ML-expansion can be given explicitly, see [32] or Appendix C. Motivated by this theorem Weiss chooses the Ansatz

$$S(k) = S_{\mathrm{bg}}(k) + \sum_m \frac{\mathcal{R}_m}{k - k_m} \,. \tag{4.18}$$

The term $\sum_m \frac{\mathcal{R}_m}{k-k_m}$ contains the prescribed poles, k_m, and residues, $\mathcal{R}_m$. The 'background' term, $S_{\mathrm{bg}}(k)$, constitutes some entire rest, i.e., it has no poles. Weiss does *not* present a way to calculate the background solely based on the information of the QNMs. It is, however, assumed that the background is sufficiently smooth. This allows for a polynomial fit by computing the S-matrix through other methods at a couple of reference points spread across the spectrum. Despite the background-fit being computationally cheap, it prevents Weiss' approach to achieve the—maybe overly ambitious—goal of finding a semi-analytical expansion of the S-matrix without any fit parameters. Again, it might be conceivable to incorporate Domcke's theory in order to express even the background in terms of QNMs (cf. section 4.2.2).

Before we turn our attention to the calculation of the residues $\mathcal{R}_m$, we need to discuss the partition of the total field into a background and a scattered component. Consider the HE (with appropriate boundary conditions) that describes our scattering process:

$$\hat{D}\,\mathbb{F}(\mathbf{r};k) \coloneqq \nabla \times \nabla \times \mathbb{F}(\mathbf{r};k) - \varepsilon(\mathbf{r};k)k^2\mathbb{F}(\mathbf{r};k) = 0\,.$$

$\hat{D}$ is the differential operator describing the HE[14] and for our scattering problems $\varepsilon(\mathbf{r};k) = \varepsilon_{\mathrm{bg}} + \Delta\varepsilon(\mathbf{r};k)$, where $\varepsilon_{\mathrm{bg}}$ is the constant dielectric permittivity of the medium that embeds our scattering region. Inside the scattering region $\Delta\varepsilon(\mathbf{r};k) \neq 0$, in the exterior $\Delta\varepsilon(\mathbf{r};k) = 0$. Next, we make the ansatz

$$\mathbb{F} = \mathbb{F}_{\mathrm{bg}} + \mathbb{F}_{\mathrm{scat}}\,. \tag{4.19}$$

The background field $\mathbb{F}_{\mathrm{bg}}$ is defined to be the part of the total field that solves the HE for $\varepsilon(\mathbf{r};k) = \varepsilon_{\mathrm{bg}}$; as if there was no scattering region at all, only free space. For our purposes it is always generated by a single active channel carrying some input state $\mathbb{I}_N$ but it contains outgoing waves as well[15]. The scattered field is the result of the incoming wave interacting with the scattering region.

[14] $\hat{D}$ is the analogue to the Maxwell-operator $\hat{\mathbb{M}}$ in [36].

[15] Consider, for instance, the one-dimensional case where an incoming wave from the left propagates through the scattering region to the right and becomes an outoing wave.

Inserting Equation (4.19) into the HE, doing some rearranging and utilising that $\mathbb{F}_{\mathrm{bg}}$ fulfils the HE for $\varepsilon(\mathbf{r};k)=\varepsilon_{\mathrm{bg}}$ we get

$$\hat{D}\,\mathbb{F}_{\mathrm{scat}}(\mathbf{r};k)=\Delta\varepsilon(\mathbf{r};k)k^2\mathbb{F}_{\mathrm{bg}}(\mathbf{r};k)\,, \tag{4.20}$$

which is a non-homogeneous HE: $\mathbb{F}_{\mathrm{bg}}$, impinging on the scattering region described by $\Delta\varepsilon(\mathbf{r};k)$, gives rise to the source term (the right-hand side) which produces the scattered field $\mathbb{F}_{\mathrm{scat}}$.

Equation (4.20) can be solved inside the scattering region with the 'inverse' of $\hat{D}$: the Green's function $G(\mathbf{r},\mathbf{r}';k)$. At this point the QNMs come into play since the Green's function can be ML-expanded in the interior [31] and takes the form

$$G(\mathbf{r},\mathbf{r}';k)=\sum_m \frac{\varphi_m(\mathbf{r})\otimes\varphi_m^{\mathrm{R}}(\mathbf{r}')}{2k_m(k-k_m)}=\sum_m \frac{\varphi_m(\mathbf{r})\otimes\varphi_m(\mathbf{r}')}{2k_m(k-k_m)}\,, \tag{4.21}$$

where $\varphi_m(\mathbf{r})$ is the scalar field of the m^{th} QNM, $\otimes$ is the outer product[16], k_m is the m^{th} QNM-wavenumber and the superscript R denotes the reciprocal state. These reciprocal states will not play a role for our waveguide geometries where $\varphi_m^{\mathrm{R}}(\mathbf{r})=\varphi_m(\mathbf{r})$[17]. After solving (4.20) for $\mathbb{F}_{\mathrm{scat}}$ by employing the ML-expansion of the Green's function we obtain

$$\begin{aligned}\mathbb{F}_{\mathrm{scat}}&=\Delta\varepsilon(\mathbf{r};k)k^2\hat{G}(\mathbf{r},\mathbf{r}';k)\mathbb{F}_{\mathrm{bg}}(\mathbf{r};k)=\\&=\sum_m \frac{\varphi_m(\mathbf{r})\otimes\langle\varphi_m(\mathbf{r}')|\mathbb{F}_{\mathrm{bg}}(\mathbf{r};k)\rangle_{\mathcal{V}}}{2k_m(k-k_m)}\,.\end{aligned} \tag{4.22}$$

4.3.3. Residues of the Scattering Matrix

We now possess the tools to find the residues $\mathcal{R}_m$ which are actually matrices with entries

$$\mathcal{R}_{m,\,NN'}=\operatorname*{Res}_{k=k_m} S(k)_{NN'}=\operatorname*{Res}_{k=k_m} S(k)_{NN'}\alpha^{\mathrm{in}}_{N'}(k)=\operatorname*{Res}_{k=k_m}\alpha^{\mathrm{out}}_{N}(k)\,. \tag{4.23}$$

Keep in mind that the last equality in (4.23) holds in the context of only one incoming channel N' being active. Substituting the ansatz (4.19) for the total field in the definition of α^{out}_N, Equation (4.17), and expressing the scattered field

[16] In bra-ket notation, $\varphi_m(\mathbf{r})\otimes\varphi_m(\mathbf{r}')$ becomes $\int\int|\mathbf{r}\rangle\langle\mathbf{r}|\varphi_m\rangle\langle\varphi_m^*|\mathbf{r}'\rangle\langle\mathbf{r}'|\,\mathrm{d}\mathbf{r}\mathrm{d}\mathbf{r}'$.

[17] This is due to the fact that incoming waveguide modes form a standing wave between the waveguide walls in y-direction of the form $\sin(yn\pi/L)\propto e^{ik_y y}-e^{-ik_y y}$, where $e^{-ik_y y}$ is the reciprocal state of $e^{ik_y y}$. Thus, the waveguide always carries the state in superposition with its reciprocal which renders the distinction irrelevant. In general, one has to take reciprocal states into account, cf. [24, 36].

through (4.22) we get

$$\alpha_N^{\text{out}}(k) = \\ [\mathbb{I}_N(\mathbf{r};k)|\mathbb{F}_{\text{bg}}(\mathbf{r};k)]_{\partial\mathcal{V}} + \sum_m \frac{[\mathbb{I}_N(\mathbf{r};k)|\varphi_m(\mathbf{r})]_{\partial\mathcal{V}}\,\langle\varphi_m(\mathbf{r}')|\mathbb{F}_{\text{bg}}(\mathbf{r};k)\rangle_{\mathcal{V}}}{2k_m(k-k_m)}\,. \quad (4.24)$$

As the first term of the right-hand side in (4.24) does not contain any poles the residues are

$$\mathcal{R}_{m,\,NN'} = \operatorname*{Res}_{k=k_m} \alpha_N^{\text{out}}(k) = \\ = \frac{1}{2k_m}\,[\mathbb{I}_N(\mathbf{r};k_m)|\varphi_m(\mathbf{r})]_{\partial\mathcal{V}}\,\langle\varphi_m(\mathbf{r}')|\mathbb{F}_{\text{bg},\,N'}(\mathbf{r};k_m)\rangle_{\mathcal{V}}\,, \quad (4.25)$$

where $\mathbb{F}_{\text{bg},\,N'}$ is the background field that arises due to a singly active incoming state $\mathbb{I}_{N'}$. Notice, that $\mathcal{R}_m$ does not depend on k, only on k_m. Furthermore, we need to identify an analytic continuation of the basis states $\mathbb{I}_N(\mathbf{r};k)$ for complex valued k [36]. For the plane-waves representing our waveguide modes this is as simple as setting $k = k_m$.

If Green's second identity holds, one can further simplify the expression for the residues in (4.25) [36]

$$\boxed{\mathcal{R}_{m,NN'} = -\frac{1}{2k_m}\,[\mathbb{I}_N(\mathbf{r},k_m)|\varphi_m(\mathbf{r})]_{\partial\mathcal{V}}\;\;[\varphi_m(\mathbf{r})|\mathbb{I}_{N'}(\mathbf{r},k_m)]_{\partial\mathcal{V}}}\,. \quad (4.26)$$

We can now insert the residues into the ansatz (4.18), fit the background term $S_{\text{bg}}(k)$ and finally obtain the sought after expansion of the S-matrix. Aside from the background, it merely depends on the QNM-fields on the surface of the scattering region[18] and the complex QNM wavenumbers k_m. The results for the quantum mechanical one-dimensional Fabry-Pérot will be presented in Section 4.3.5.

4.3.4. Normalisation of the Quasi-Normal Modes

There remains one important aspect we did not discuss so far: the QNMs, $\varphi_m(\mathbf{r})$, have to be properly normalised. There have been many attempts to formulate such a normalisation, see the appendix of [45] for a critical juxtaposition. Nonetheless, for the ML-expansion of the Green's function (4.21) we require the normalisation presented in [45][19] which is a simplified version of a more general form; for periodic

[18] At this point it might seem that Weiss' approach, just like Alpeggiani's, only requires the far-field information. Nonetheless, the QNMs need to be normalised which cannot be done without the QNM field *inside* the scattering region.

[19] An equivalent formulation can also be found in much earlier works, e.g., in the context of quantum mechanics, see the appendix of [51].

structures solved in the context of the HE see [24] and for the most general case of Maxwell's equations see [25].

We briefly comment on how the normalisation is derived: assuming the ML-expansion of the Green's function for the scattered field given in Equation (4.21) holds, the idea is to solve a non-homogeneous HE for some real k and some source term $\sigma(\mathbf{r};k)$: $\mathbb{F}(\mathbf{r};k) = \int G(\mathbf{r},\mathbf{r}';k)\sigma(\mathbf{r};k)\mathrm{d}\mathbf{r}'$. Then, we continue the solution by making k complex and steering it towards one of the k_m. Simultaneously, we diminish the source term progressively until it is turned off as soon as $k = k_m$, i.e., $\sigma(\mathbf{r};k) = (k^2 - k_m^2)\hat{\sigma}(\mathbf{r})$ in the vicinity of k_m. Thus, the continued solution will become the m^{th} QNM[20]:

$$\begin{aligned}\varphi_m(\mathbf{r}) &= \lim_{k\to k_m} \int G(\mathbf{r},\mathbf{r}';k)\sigma(\mathbf{r};k)\mathrm{d}\mathbf{r}' = \varphi_m(\mathbf{r})\,\langle\varphi_m(\mathbf{r}')|\hat{\sigma}(\mathbf{r})\rangle_{\mathcal{V}} \\ &\implies \langle\varphi_m(\mathbf{r}')|\hat{\sigma}(\mathbf{r})\rangle_{\mathcal{V}} \overset{!}{=} 1\,.\end{aligned}$$

We can express $\hat{\sigma}$ via the original HE, $\hat{\sigma} = \lim_{k\to k_m} \hat{D}\,\mathbb{F}/(k^2 - k_m^2)$, and we obtain, after some algebraic manipulations,

$$\left[\varphi_m(\mathbf{r})\left|\frac{\partial\widetilde{\varphi}_m(\mathbf{r};k)}{\partial(k^2)}\right|_{k=k_m}\right]_{\partial\mathcal{V}} + \left\langle\varphi_m(\mathbf{r})\left|\frac{\partial(k^2\varepsilon(\mathbf{r};k))}{\partial(k^2)}\right|_{k=k_m}\varphi_m(\mathbf{r})\right\rangle_{\mathcal{V}} = 1\,,$$

where $\widetilde{\varphi}_m$ is the continued solution near the pole k_m. It should be obvious that the normalisation is not trivial and, most importantly, requires the knowledge of the QNMs *inside* the scattering region. This fact is in stark contrast to Alpeggiani's normalisation-free method, that, nonetheless, does not work for our complex waveguide, on which we, unfortunately, could not test Weiss' approach since a corresponding implementation would have gone beyond the scope of this work.

4.3.5. Results for the One-Dimensional Fabry-Pérot

To see whether or not Weiss' method could be adapted for our needs, we applied it to solve the Schrödinger Equation (SE) for scattering on the one-dimensional Fabry-Pérot cavity (1DFP). The solution is entirely analytical, including the background term. This allowed us to obtain a thorough understanding of the formalism which we hoped, could explain the peculiar results obtained through Salihbegović's unitarity correction. Unfortunately, this was not the case but Weiss' approach appears to be a superior alternative with respect to the quality of reconstruction—at least for this simple example. The detailed derivation can be found in Appendix C.

[20] In our description the source term is a direct consequence of the incoming field (cf. Equation (4.20)). If the source turns off when $k = k_m$, the incoming field consequently vanishes and the (non-trivial) solution for this case is thus, per definition, a QNM.

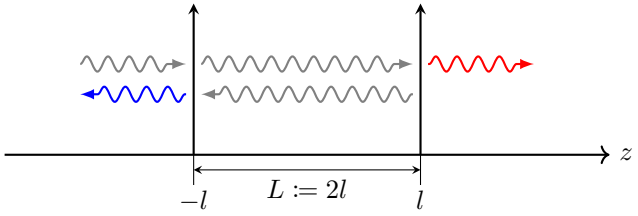

Figure 4.7.: Schematic of the one-dimensional Fabry-Pérot for an incoming wave from the left. The potential consists of two Dirac deltas with weight γ that are separated by a length L. The deltas act as semi-transparent mirrors making up a cavity.

Even though we presented Weiss' approach in the context of the HE, we can easily apply it to the SE as both equations are—to a certain degree—equivalent [39]: a quantum-mechanical potential $V(\mathbf{r})$ translates to a dispersive medium, i.e., the equivalent permittivity is k-dependent: $\varepsilon(\mathrm{r}; k) = 1 - 2V(\mathrm{r})/k^2$. For the 1DFP, sketched in Figure 4.7, $V(z) = \gamma(\delta(z + l) + \delta(z - l))$. While the 'translation' of the potential is straightforward, the Dirac delta functions do not comply with Green's second identity. Thus, we had to resort to Equation (4.25) for expressing the residues $\mathcal{R}_m$ instead of Equation (4.26).

The left column of Figure 4.8 depicts the transmission and reflection (top) as well as their phases (bottom) obtained by Weiss' expansion with 2×10 QNMs: 10 QNMs with real parts greater than zero, $k_{m>0}$, plus their mirrored counterparts, $k_{m<0} = -k^*_{m>0}$. Not including the mirrored QNMs leads to non-unitary and thus wrong results. The reconstructed transmission's and reflection's deviation from the analytical reference (grey) is barely visible up to $k = 1000$. Even the phase is matched accurately in that range.

For comparison, we applied Salihbegović's reconstruction to the 1DFP. Note that Salihbegović's expansion is defined over energy which is proportional to k^2. Consequently, for a given QNM-energy E_m, we cannot determine whether or not the corresponding QNM-wavenumber, $k_m \propto \pm\sqrt{E_m}$, is that of a pole (usual QNM) or a zero (time-reversed QNM): from the energy-perspective the k-plane overlaps with itself such that the zeros of the second quadrant lie exactly on top of the poles from the fourth quadrant on another Riemann sheet. Likewise, the (mirrored) poles from the third quadrant lie on top of the zeros from the first quadrant. For the expansion we need to choose the QNM-energies that correspond to the QNM-wavenumbers from the *physical sheet*, i.e., the sheet containing solutions for outgoing boundary conditions, see [6] or cf. [44]. These energies have positive real parts and negative imaginary parts. As there are no mirrored counterparts, only half the amount of poles used in Weiss' expansion is used here.

As seen from the right column of Figure 4.8, Salihbegović's reconstructed transmission and reflection are slightly worse than Weiss' with 10 QNMs. The phase seems to be offset and exhibits a jump for the transmission amplitude around $k \approx 125$. Increasing the amount of QNMs to 2×20 or 20, Figure 4.9, further improves the reconstruction in both cases as expected. For 2×60, Figure 4.10, Weiss' reconstruction can no longer be distinguished from the analytical reference, unlike Salihbegovic's method, which, however, seems to approach perfect reconstruction. Note, that the phase jump vanished. Further increasing to 2×160 QNMs, Figure 4.11, does not change the results of Weiss' expansion anymore. While Salihbegovic's transmission and reflection spectra still improve, the phase worsens, seemingly converging to a constant offset from the true value. As this discrepancy remains unexplained, it could point to a fundamental problem of the expansion related to the issues discussed in Section 4.2.

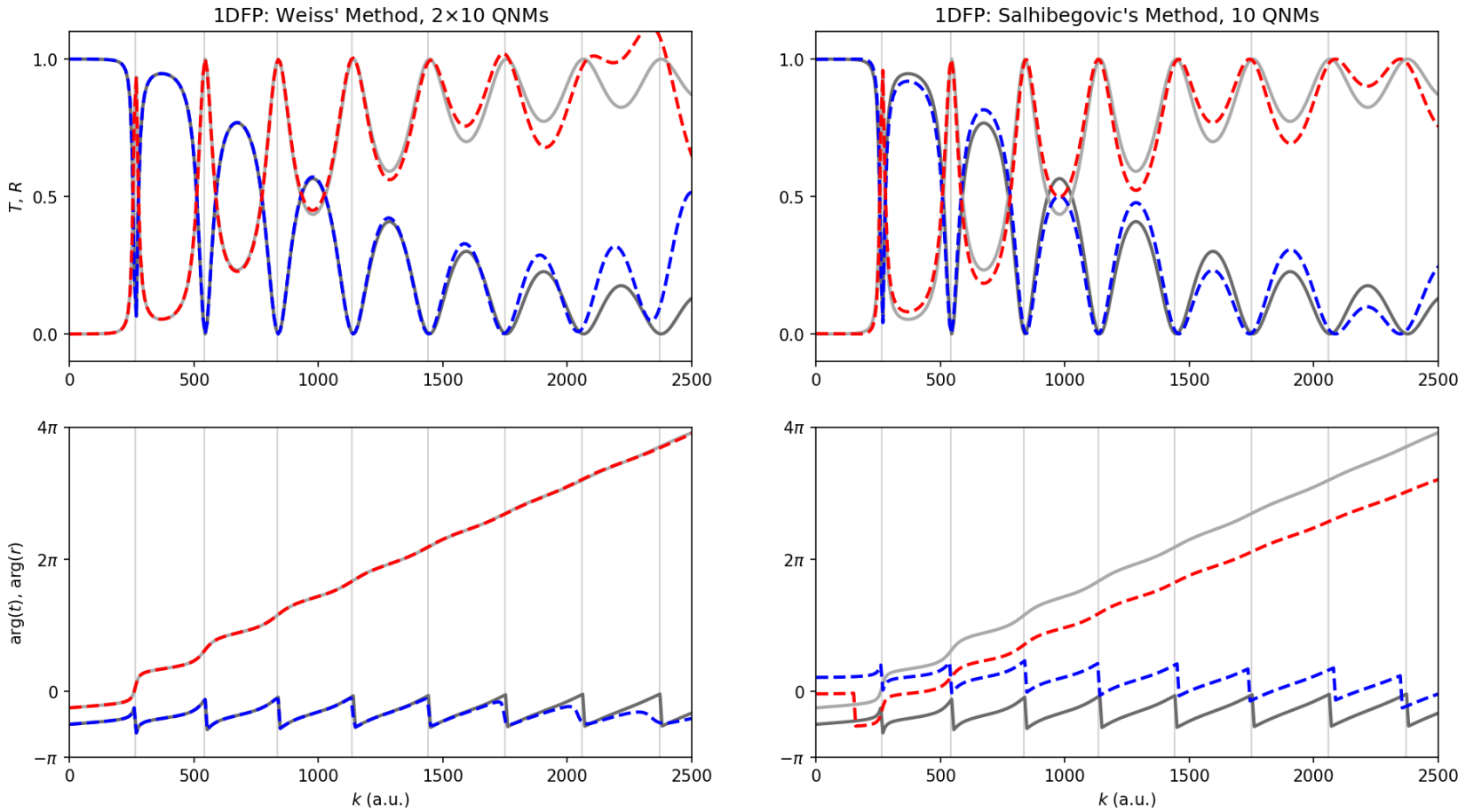

Figure 4.8.: Weiss' method with 2×10 QNMs on the left, Salihbegovic's method with 10 QNMs on the right. Reference in grey, transmission in red and reflection in blue; absolute-squares on top, phase at the bottom. Vertical lines mark the positions of the QNMs. We sampled the cavity with $N_z = 101$ points with a spacing of $\Delta z = 1 \times 10^{-4}$. The Dirac deltas were positioned at the first and last point with a weight of $\gamma = 5 \times 10^6/\Delta z$. Clearly, the reconstruction works very well for small k. For larger k, more QNMs are necessary for an accurate reconstruction, see Figure 4.9.

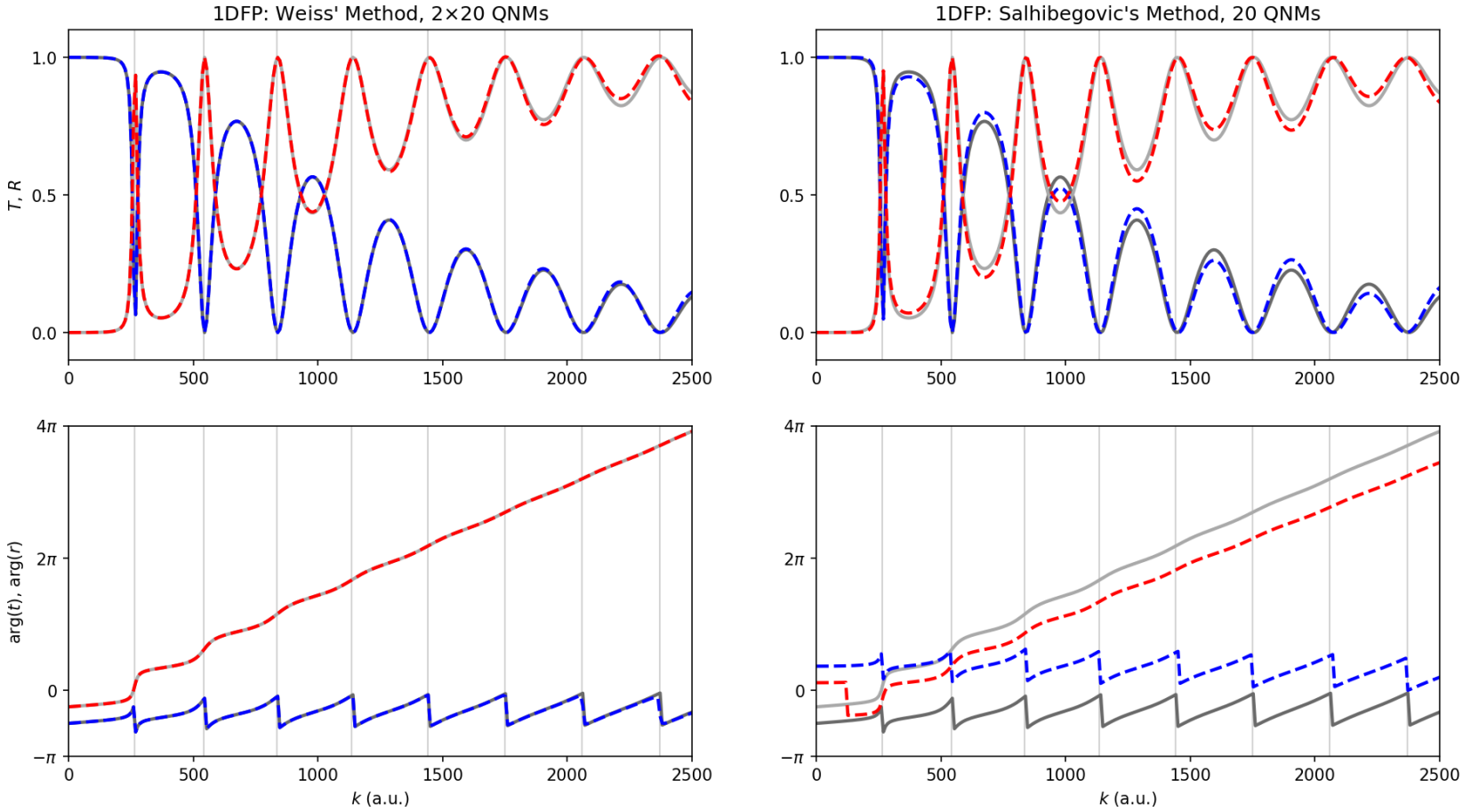

Figure 4.9.: By doubling the amount of QNMs, as compared to Figure 4.8, Weiss' reconstruction is almost perfect over the shown spectrum. Salihbegović's reconstruction improves but especially the phase is not reconstructed accurately.

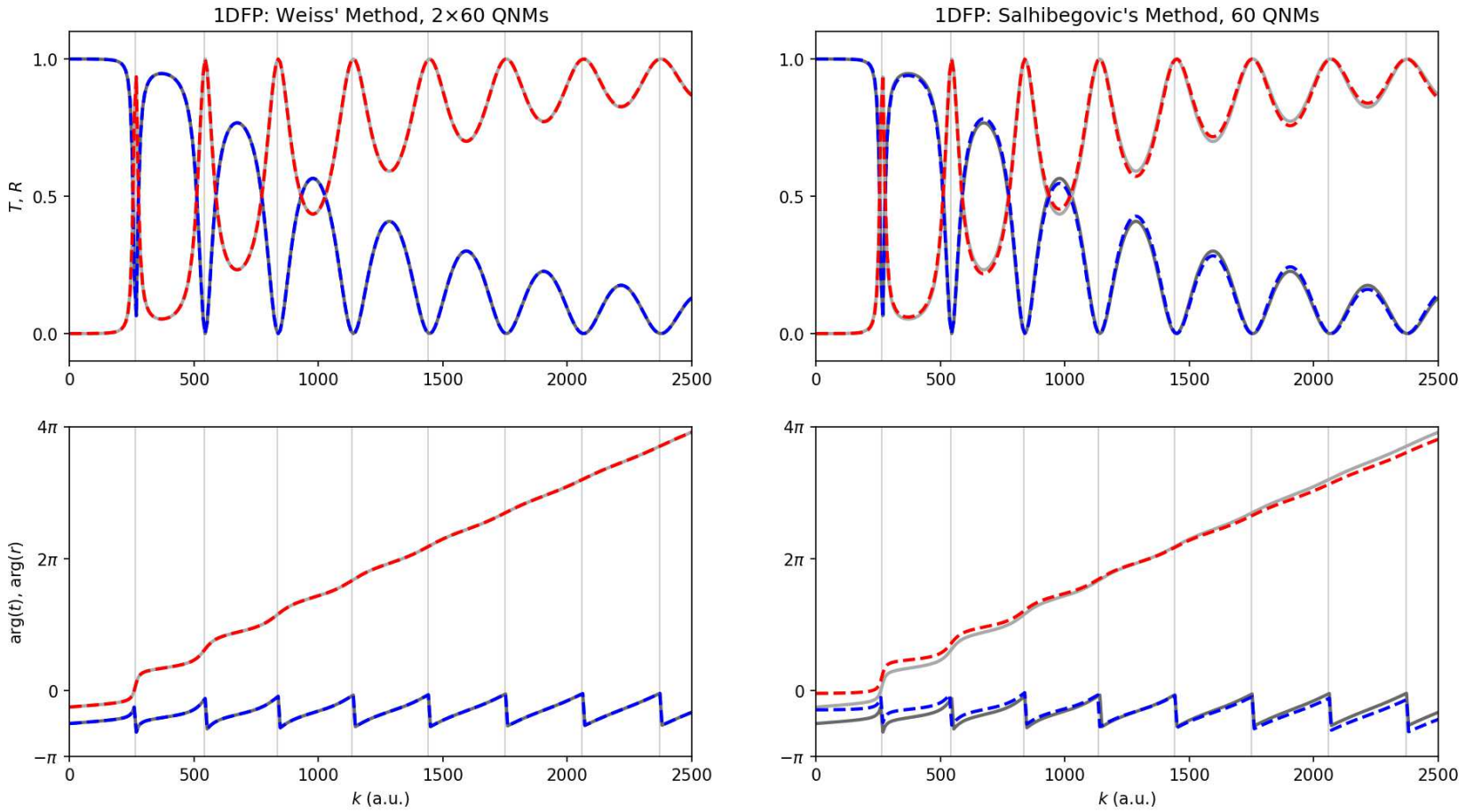

Figure 4.10.: With 2×60 QNMs, Weiss' method yields seemingly perfect results. For Salihbegović's method with 60 QNMs, visible differences to the reference remain which, however, appear to converge to zero.

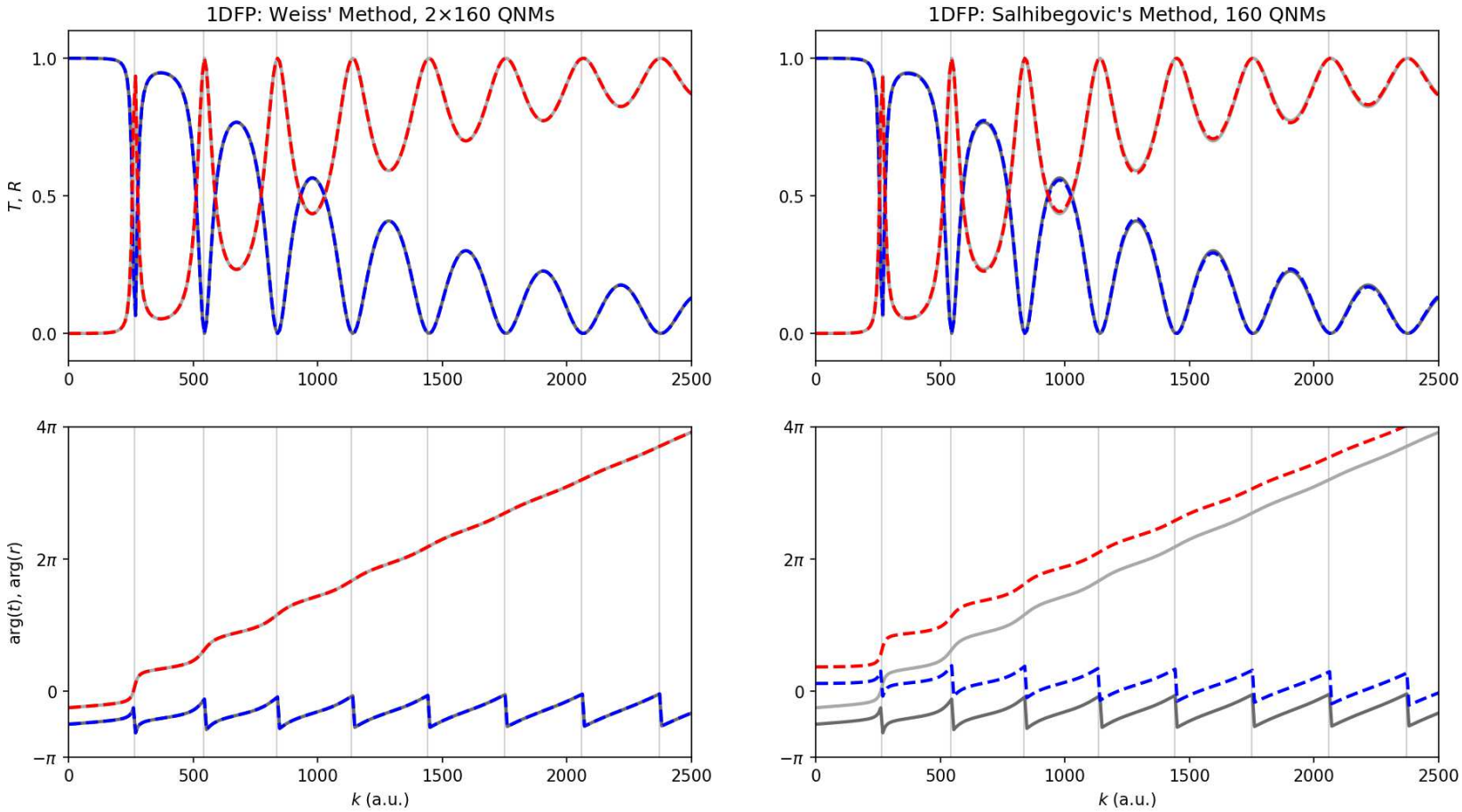

Figure 4.11.: There is no change to Weiss' already perfectly reconstructed spectrum when going from 2×60 (Figure 4.10) to 2×160 QNMs, which comes to no surprise because the QNMs that were added have large real parts and thus have no effect on the range of the shown spectrum. Salihbegović's reconstruction, on the other hand, shows further improvement, although subtle deviations are still visible. Peculiarly, the phase, that seemed to converge to the reference for less QNMs, is clearly offset.

Chapter 5.

Summary and Outlook

In this work we investigated several QNM-expansions of the S-matrix with the ambition of finding a representation depending only on the QNM far-fields without any fit-parameters. We discussed Salihbegović's work, which clearly shows that Alpeggiani's expansion [34] fails to reconstruct the S-matrix for the complex scattering system presented in Section 4.1.2: the resulting S-matrix strongly violates unitarity. Salihbegović's unitarity correction [35] to Alpeggiani's formula leads to unitary S-matrices even for highly non-symmetric scatterers and allows to accurately calculate the total transmissions and reflections. Nonetheless, the resulting S-matrix violates reciprocity and reconstructs transmission or reflection between single channels incorrectly. We attempted to explain and fix these shortcomings. We studied the effective Hamiltonian formalism and its derivation through Feshbach's projection operators: it deepened our understanding of the matter, but ultimately, we did not manage to employ the formalism to explain or resolve the issues of Alpeggiani's and Salihbegović's expansions. Likewise, other attempts to find a potentially missing background of the S-matrix, a pattern in the error terms for deriving a generally valid correction, or a connection to the Weierstrass factorisation presented in [33, 42] were unsuccessful. Finally, we turned our attention to Weiss' formalism [36] and successfully applied it to the quantum mechanical Fabry-Pérot cavity in one dimension. The resulting expansion is entirely analytical since we were able to express the QNM-wavenumbers in terms of the generalised Lambert-W function.

As the scope of this work was limited, we could not proceed with the next step, namely, testing Weiss' formalism on a more complex scattering geometry, for which Salihbegović's approach only partially succeeded. In order to do so, one would need to normalise the QNMs of the system, which requires the QNM-wavefunctions inside the scattering region. This and the need to fit the background are the main disadvantages of Weiss' method. However, it might be possible to come up with a different normalisation scheme based on the S-matrix that would only depend on the QNM far-fields as in Alpeggiani's approach. Furthermore, one could try to adapt the work of Domcke [40] and express Weiss' background term solely through QNMs without the need for a fit procedure. Generally, Domcke's publication [40]

holds some valuable pointers, for example, to another way to calculate the QNMs: the correspondence between bound states and QNMs is captured by the so-called *level-shift matrix* from which one might be able to extract the exact positions of the QNMs efficiently, especially, since one can choose through which bound states it should be represented. Choosing only one bound state at a time would make the level-shift matrix a scalar, possibly yielding a simple equation for each QNM. It might also be fruitful to review the vast literature from nuclear physics on this topic in more depth. The Humblet-Rosenfeld expansion [6, 52] might be a suitable candidate for further study as well as the works of Berggren [53, 54].

After all, the ability to efficiently calculate the QNMs and use them in a semi-analytical expansion of the S-matrix would not only speed up its calculation but also allow for deeper physical insights that cannot be brought to light by purely numerical methods. A proper QNM-expansion would describe scattering phenomena in a compact and transparent fashion with relevance to lasing theory [30], transmission eigenchannels in random media [55], the generalised Wigner-Smith operator [1], exceptional points [56] and nanophotonics [26, 57]. While there are already solid results for symmetric [33, 34] and periodic [36] systems with few resonances, several obstacles remain to be overcome after our effort to find a QNM-expansion for more complex scattering scenarios.

Appendix A.

Derivation of the Effective Hamiltonian Formula

Using the Feshbach projection formalism [51, 58] we can separate any Hamiltonian into an inner space and an outer space. The respective projection operators are Q and P for which

$$Q^2 = Q\,,$$
$$P^2 = P\,,$$

i.e., the defining property of a projection operator and

$$Q + P = \mathbb{1}\,,$$
$$QP = PQ = 0\,,$$

where $\mathbb{1}$ is the identity operator. Therefore, every wavefunction is entirely represented by its Q-space and P-space parts, $Q\,|\Psi\rangle + P\,|\Psi\rangle = |\Psi\rangle$

The P-space is chosen such that it contains the asymptotic behaviour of the incoming and scattered wavefunctions. Solving the scattering problem is thus equivalent to finding the P-space part of the wavefunction for a given input wave. The Q-space, on the other hand, contains the scattering potential and represents—on its own—a closed system.

Considering the Schrödinger Equation (SE) in a matrix representation the segmentation can be visualised as follows:

$$\underbrace{\left(\begin{array}{c|c} QHQ & QHP \\ \hline PHQ & PHP \end{array}\right)}_{H} \underbrace{\left(\begin{array}{c} Q\,|\Psi\rangle \\ \hline P\,|\Psi\rangle \end{array}\right)}_{|\Psi\rangle} = E \underbrace{\left(\begin{array}{c} Q\,|\Psi\rangle \\ \hline P\,|\Psi\rangle \end{array}\right)}_{E|\Psi\rangle}\,.$$

We define $H_{QQ} := QHQ$, $H_{PQ} := PHQ$ and so on. The blocks[1] H_{QQ} and H_{PP} describe the the Q and P parts of the Hamiltonian, respectively, while H_{PQ} and H_{QP} constitute the coupling between the scattering system and its asymptotic region. To find a scattering solution and ultimately express the S-matrix with this formalism we rewrite the SE as a pair of coupled equations:

$$(E - H_{QQ})Q\,|\Psi\rangle = H_{QP}P\,|\Psi\rangle\ , \tag{A.1}$$
$$(E - H_{PP})P\,|\Psi\rangle = H_{PQ}Q\,|\Psi\rangle\ . \tag{A.2}$$

As mentioned above we want to solve for $P\,|\Psi\rangle$. First, Equation (A.2) is rewritten as a Lippmann-Schwinger equation

$$P\,|\Psi\rangle = |\psi_0\rangle + \underbrace{(E^{(+)} - H_{PP})^{-1}}_{=:G_P^{(+)}} H_{PQ}Q\,|\Psi\rangle\ , \tag{A.3}$$

where ψ_0 and $G_P^{(+)}$ are the free wave and the Green's function in P-space, respectively. Reinserting into (A.1) gives

$$\begin{aligned}(E - H_{QQ})Q\,|\Psi\rangle &= H_{QP}\,|\psi_0\rangle + H_{QP}G_P^{(+)}H_{PQ}Q\,|\Psi\rangle \\ \Rightarrow Q\,|\Psi\rangle &= (E - H_{QQ} - H_{QP}G_P^{(+)}H_{PQ})^{-1}H_{QP}\,|\psi_0\rangle\ .\end{aligned}$$

Using the expression for $Q\,|\Psi\rangle$ in Equation (A.3) finally yields

$$P\,|\Psi\rangle = |\psi_0\rangle + G_P^{(+)}H_{PQ}(E - H_{QQ} - H_{QP}G_P^{(+)}(E)H_{PQ})^{-1}H_{QP}\,|\psi_0\rangle\ . \tag{A.4}$$

The term $H_{\text{eff}} := H_{QQ} + H_{QP}G_P^{(+)}H_{PQ}$ is known as the effective Hamiltonian. It couples the 'closed system' H_{QQ} to the continuum, i.e. the P-space, via $H_{QP}G_P^{(+)}H_{PQ}$. Taking the inverse yields the 'effective' Green's function which describes the propagation through the scattering region. $P\,|\Psi\rangle$ in Equation (A.4) is the sum of the input wave $|\psi_0\rangle$ and the scattered wave $G_P^{(+)}H_{PQ}G_{\text{eff}}H_{QP}\,|\psi_0\rangle$ which couples to the Q-space via H_{PQ} where it is scattered (G_{eff}), coupled out again (H_{PQ}) and is finally propagated as an outgoing wave through P-space via $G_P^{(+)}$.

The Green's function $G_P^{(+)}$ in the coupling term can be expanded [29]:

$$\begin{aligned}H_{QP}G_P^{(+)}H_{PQ} &= \sum_n \int_{\varepsilon_n}^{\infty} \frac{H_{QP}\,|k',n\rangle\,\langle k',n|\,H_{PQ}}{(E + i0) - E'}\mathrm{d}E' = \\ &= \sum_n \mathcal{P}\int_{\varepsilon_n}^{\infty} \frac{H_{QP}\,|k',n\rangle\,\langle k',n|\,H_{PQ}}{E - E'}\mathrm{d}E' - i\pi H_{QP}\,|k,n\rangle\,\langle k,n|\,H_{PQ}\,,\end{aligned}$$

[1] All blocks are typically of infinite size.

where the integral was evaluated by the Sokhotsky-Plemelj theorem with $\mathcal{P}\int\cdot\,\mathrm{d}E'$ the Cauchy principal value. ε_n is the minimum channel energy[2] and $|k,n\rangle$ is a free wave in P-space and channel n. We assume that all matrix elements of $H_{QP}\,|k',n\rangle\,\langle k',n|\,H_{PQ}$ qualify as complex functions $\chi(E')$ ($k'=k(E')$) for which the Kramers-Kronig relations hold. Then[3]

$$-\pi\mathrm{Re}\{\chi(E)\}=\mathcal{P}\int_{-\infty}^{\infty}\frac{\mathrm{Im}\{\chi(E')\}}{E-E'}\mathrm{d}E'\,,$$
$$\pi\mathrm{Im}\{\chi(E)\}=\mathcal{P}\int_{-\infty}^{\infty}\frac{\mathrm{Re}\{\chi(E')\}}{E-E'}\mathrm{d}E'\,,$$

and we see that $\chi(E)=-H_{QP}G_P^{(+)}H_{PQ}/\pi$ splits into its real and imaginary part while prescribing the latter:

$$\begin{aligned}H_{QP}G_P^{(+)}H_{PQ}&=\sum_n-\pi\mathrm{Re}\{\chi(E)\}_n-i\pi\mathrm{Im}\{\chi(E)\}_n=\\&=\sum_n-\pi\mathrm{Re}\{\chi(E)\}_n-\frac{i}{2}W_nW_n^\dagger\,,\end{aligned}\tag{A.5}$$

with $W_n=\sqrt{2\pi}H_{QP}\,|k,n\rangle$ and $W_n^\dagger=\sqrt{2\pi}\,\langle k,n|\,H_{PQ}$.

The S-matrix is given by $S_{mn}=\delta_{mn}-2\pi iT_{mn}$ [59]. The on-shell T-matrix elements in the channel representation follow immediately from Equation (A.4)

$$T_{mn}=\langle k,m|\,H_{PQ}(E-H_{QQ}-H_{QP}G_P^{(+)}H_{PQ})^{-1}H_{QP}\,|k,n\rangle\,,$$

and hence we obtain

$$\begin{aligned}S_{mn}&=\delta_{mn}-2\pi i\,\langle k,m|\,H_{PQ}(E-H_{QQ}-H_{QP}G_P^{(+)}H_{PQ})^{-1}H_{QP}\,|k,n\rangle\\&=\delta_{mn}-iW_m^\dagger(E-H_{QQ}+\pi\mathrm{Re}\{\chi(E)\}+\frac{i}{2}WW^\dagger)^{-1}W_n\end{aligned}$$

$$\boxed{S_{mn}=\delta_{mn}-iW_m^\dagger\frac{1}{E-H_{\mathrm{eff}}}W_n\,.}\tag{A.6}$$

($W=(W_1\ \ W_2\ \ W_3\ \ ...)$ is the matrix containing all W_n as columns.)

[2]The energy below which the channel is closed.
[3]Be aware of the swapped sign in the denominator when comparing to the usual formulation.

A.1. Demonstration: a Discrete Example

To see how this works for the discrete case consider a 1D example-Hamiltonian in its tridiagonal form (in coordinate representation). By 'removing' two off-diagonal elements we separate the Q- and the P-space.

$$H = -\underbrace{\frac{1}{2\Delta z^2}}_{=t} \left(\begin{array}{ccc|ccc} & & & & & \\ \multicolumn{3}{c|}{\overset{H_{QQ}}{\ddots}} & \multicolumn{3}{c}{\overset{H_{QP}}{}} \\ 1 & -2 & 1 & & & \\ & 1 & -2 & 1 & & \\ \hline & & 1 & -2 & 1 & \\ & & & 1 & -2 & 1 \\ \multicolumn{3}{c|}{\underset{H_{PQ}}{}} & \multicolumn{3}{c}{\underset{H_{PP}}{\ddots}} \end{array} \right)$$

H_{PP} is then equivalent to the Hamiltonian of a semi-infinite lead.

Keep in mind that whenever we handle *discrete* Green's functions we need to multiply by the step width Δz since in the discrete case

$$(E - H)G = \frac{\mathbb{1}}{\Delta z}\,.$$

Thus, the proper impulse response for some discrete Hamiltonian H will be the discrete Green's function accompanied by an extra Δz: $\widetilde{G} = G\Delta z$. As a consequence Equation (A.6) has to be altered slightly:

$$S = \mathbb{1} - i\widetilde{W}^{\dagger} G_{\text{eff}} \Delta z \widetilde{W}\,,$$

where the discrete coupling matrix has to be changed according to $W = \sqrt{\Delta z}\,\widetilde{W}$. This also holds for the W contained in G_{eff} as will be shown below.

Now, by inspecting the discrete version of our coupling term, $H_{QP} G_P^{(+)} \Delta z H_{PQ}$, we see that the Green's function needs evaluation only at a single point namely on the border of the Q-space. This is due to the single non-zero entry $-t \cdot 1$ in the coupling matrices H_{QP} and H_{PQ}. With the discrete Green's function for the semi-infinite lead at the border $G_P^{(+)}(z = z_{P,0}, z' = z_{P,0}) = -\frac{e^{ik\Delta z}}{t\Delta z}$ [60] we get

$$\begin{aligned} \left(H_{QP} G_P^{(+)} \Delta z H_{PQ} \right)_{z_{P,0}, z_{P,0}} &= (-t)(-\frac{e^{ik\Delta z}}{t\Delta z})\Delta z(-t) = \\ &= -t\frac{e^{ik\Delta z}}{\Delta z}\Delta z\,, \end{aligned} \tag{A.7}$$

which is exactly the boundary condition $-te^{ik\Delta z}$ we add to the 'closed' Hamiltonian at $(z = z_{P,0}, z' = z_{P,0})$ for opening it up. Furthermore, we can determine the

coupling matrices by comparing the imaginary part of (A.7) with that of (A.5) and obtain

$$H_{\text{eff}} = H_{QQ} + \text{Re}\{H_{QP}G_P^{(+)}H_{PQ}\}\Delta z + i\underbrace{\text{Im}\{H_{QP}G_P^{(+)}H_{PQ}\}\Delta z}_{\stackrel{!}{=}-1/2WW^\dagger}$$

$$\Rightarrow W_{z_{P,0},z_{P,0}} = \sqrt{\frac{\sin(k\Delta z)}{\Delta z^2}}\,,$$

and finally

$$S = \mathbb{1} - iW^\dagger G_{\text{eff}} W =$$
$$= \mathbb{1} - iW^\dagger \frac{1}{E - H_{QQ} + \text{Re}\{H_{QP}G_P^{(+)}H_{PQ}\}\Delta z - \frac{i}{2}WW^\dagger} W\,.$$

This expression for the S-matrix matches that given by Ambichl [17] —disregarding a global phase of $e^{i\pi}$—even though the Ws are defined differently. However, our formulation does not require 'arbitrary' additions of Δzs to the numerator in order to get the dimensions right.

Appendix B.

Analytical Solution for the 1D Fabry-Pérot

The one-dimensional Fabry-Pérot (1DFP) is depicted in Figure B.1. We will calculate the analytical scattering matrix by calculating the reflection and transmission amplitudes under an incoming plane wave from the left, $A\exp(ikz)$, with $A = 1$. We choose the typical ansatz:

$$\psi(z) = \begin{cases} e^{ikz} + Be^{ik-z} & z < -l \\ Ce^{ikz} + De^{ik-z} & -l < z < l \\ Ee^{ikz} & z > l \end{cases} . \tag{B.1}$$

In order to calculate the unknowns (B, C, D and E) we require the solution to be continuous. On the other hand, by integrating the Schrödinger equation over an infinitesimal range around the Dirac delta we see that the derivative of the

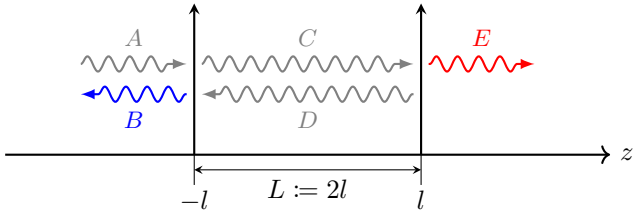

Figure B.1.: Schematic of the one-dimensional Fabry-Pérot. The potential consists of two Dirac deltas with weight γ that are separated by some length L. They act as semi-transparent mirrors which make up a cavity. The letters correspond to the complex amplitudes of the incoming, A, the reflected, B, the transmitted, E, as well as the interior, C and D, plane waves.

solution must jump at that point (after setting $\hbar = m = 1$):

$$\frac{\partial\psi}{\partial z}\left(l^+\right) - \frac{\partial\psi}{\partial z}\left(l^+\right) = 2\gamma\psi(l)\,,$$

with $l^\pm = \lim_{\varepsilon\to 0} l \pm \varepsilon$.

Combining the continuity and discontinuity conditions we arrive at the following linear system of equations for the amplitudes

$$\begin{aligned} A + B &= C + D\,, \\ ik\left(C - D - (A - B)\right) &= 2\gamma\left(A + B\right)\,, \\ Ce^{iLk} + De^{-iLk} &= Ee^{iLk}\,, \\ ik\left(Ee^{iLk} - (Ce^{iLk} - De^{-iLk})\right) &= 2\gamma\left(Ce^{iLk} + De^{-iLk}\right)\,, \end{aligned}$$

which is easily solved, e.g., with a computer algebra system like Maxima[1]. The transmission amplitude is then given by $t(k) = \frac{E}{A} = E$ and the reflection amplitude is given by $r(k) = \frac{B}{A} = B$, i.e.,

$$t(k) = \frac{k^2}{\gamma^2\left(e^{2iLk} - 1\right) + k^2 + 2i\gamma k}\,, \tag{B.2}$$

$$r(k) = -\frac{i\gamma k\left(e^{2iLk} + 1\right) + \gamma^2\left(e^{2iLk} - 1\right)}{\gamma^2\left(e^{2iLk} - 1\right) + k^2 + 2i\gamma k}\,, \tag{B.3}$$

which are arranged as the entries of the S-matrix as

$$S(k) = \begin{pmatrix} r(k) & t(k) \\ t(k) & r(k) \end{pmatrix}\,,$$

since the reflection and transmission amplitudes are equal on both sides due to symmetry.

[1] `http://maxima.sourceforge.net/`

Appendix C.

Derivation of Weiss' S-Matrix Expansion for the 1D Fabry-Pérot

In order to expand the S-matrix as $S = S_{\text{bg}} + \sum_m \frac{\mathcal{R}_m}{k-k_m}$, we need to find the Quasi-Normal Modes (QNMs) for the given problem. For the one-dimensional Fabry-Pérot (1DFP), see Figure B.1, we obtain the wavenumbers k_m of the QNMs as the solutions of (B.1) for $A = 0$, i.e., we are looking for solutions that fulfil purely outgoing boundary conditions.

Due to the lack of an incoming wave, the problem is symmetric under the parity transformation $z \to -z$. As a consequence, solutions are either even $\psi(z) = \psi(-z)$ or odd $\psi(z) = -\psi(-z)$. Thus, we make the ansatz:

$$\psi(z) = \begin{cases} \pm N e^{ik-z} & z < -l \\ D e^{ikz} \pm D e^{ik-z} & -l < z < l \\ N e^{ikz} & z > l \end{cases} . \tag{C.1}$$

Using the same continuity and jump conditions as in Appendix B and after some algebraic manipulations of the ensuing system of equations we eventually arrive at the transcendent equation determining k_m:

$$e^{ikL} = \pm\left(ik/\gamma - 1\right) , \tag{C.2}$$

where the choice of the plus or minus sign corresponds to the even or odd case, respectively. The solutions k_m are [61]

$$ik_m = \gamma - \frac{1}{L} W_{-\lfloor \frac{m}{2}+1 \rfloor}\left(-(-1)^m L\gamma e^{L\gamma}\right) \qquad \forall m \in \mathbb{Z} \setminus \{-1\} ,$$

where $W_n(\cdot)$ is the nth branch of the generalised Lambert-W function. Even and odd solutions correspond to even and odd m, respectively. The index $m = -1$ is excluded because $k_{-1} = 0$([1]). Also note that for indices $m \geq 0$, the k_m have positive real parts, while negative indices indicate negative real parts. Of course, all imaginary parts are negative as follows from the definition of the QNMs.

[1] This can be seen by using the defining equation of the real-valued Lambert-W function $W_0(x)e^{W_0(x)} = x$ and inserting accordingly into (C.2).

C.1. Weiss Formalism for the Helmholtz Equation

The Weiss formalism for Maxwell's equations [36] can be formulated for the one-dimensional[2] Helmholtz Equation (HE)

$$\hat{D}\varphi(z,k) \coloneqq \left[\nabla^2 + \varepsilon(z,k)k^2\right]\varphi(z,k) = 0 \tag{C.3}$$

as follows: the Green's function needs to be expanded as

$$\hat{G} = \sum_m \frac{\varphi_m(z) \otimes \varphi_m(z)}{2k_m(k-k_m)}\,, \tag{C.4}$$

with an additional factor $\frac{1}{2k_m}$. The bilinear 'surface' and 'volume' operators are given by:

$$\begin{aligned}\langle\varphi|\psi\rangle_{\mathcal{V}} &= \int_{\mathcal{V}} \varphi(z)\psi(z)\mathrm{d}V\,,\\ [\varphi|\psi]_{\partial\mathcal{V}} &= \int_{\partial\mathcal{V}} \varphi(z)\partial_s\psi(z) - \psi(z)\partial_s\varphi(z)\mathrm{d}S\,,\end{aligned}$$

where ∂_s is the derivative along the outward pointing surface normal. Green's second identity can then be written as

$$\left\langle \varphi \middle| \hat{D} \middle| \psi \right\rangle_V - \left\langle \psi \middle| \hat{D} \middle| \varphi \right\rangle_V = [\varphi|\psi]_{\partial V}\,.$$

The incoming and outgoing basis states defined on the surface of the minimal convex volume enclosing our scattering region must satisfy

$$\begin{aligned}\left[\varphi_N^{\mathrm{in}}|\varphi_{N'}^{\mathrm{out}}\right]_{\partial\mathcal{V}} &= \delta_{N,N'}\,,\\ \left[\varphi_N^{\mathrm{in}}|\varphi_{N'}^{\mathrm{in}}\right]_{\partial\mathcal{V}} &= \left[\varphi_N^{\mathrm{out}}|\varphi_{N'}^{\mathrm{out}}\right]_{\partial\mathcal{V}} = 0\,,\end{aligned} \tag{C.5}$$

where N is the channel index.

The QNMs φ_m are normalised according to

$$\left[\varphi_m \middle| \frac{\partial\widetilde{\varphi}_m}{\partial(k^2)}\right]_{\partial\mathcal{V}} + \left\langle \varphi_m \middle| \frac{\partial(k^2\varepsilon(z,k))}{\partial(k^2)} \middle| \varphi_m \right\rangle_{\mathcal{V}} = 1\,, \tag{C.6}$$

where $\frac{\partial\widetilde{\varphi}_m}{\partial(k^2)}$ is the derivative of φ_m's expansion into outgoing basis states, $\widetilde{\varphi}_m(k) = \sum_N \alpha_N\varphi_N^{\mathrm{out}}(k)$, with respect to k^2 evaluated at $k = k_m$.

Equations (C.3) to (C.6) are the building blocks for the Weiss formalism acting on the HE. In order to apply it to the 1DFP, we need to translate our problem

[2] Considering the 1D case simplifies the procedure: there are no reciprocal states, surface integrals reduce to a sum of two points and volume integrals correspond to line integrals.

that was originally formulated for the Schrödinger Equation (SE). This is possible due to the equivalence of the HE and the SE [39]. It follows

$$\varepsilon(z,k) = 1 - \frac{2V(z)}{k^2}\,,$$

where $V(z) = \gamma(\delta(z+l)+\delta(z-l))$ is the 1DFP-potential. Thus, the k-independent potential translates into a dispersive, i.e., k-dependent, dielectric function. Although it will not play a role in the following derivations, keep in mind that, while the equations are of the same form, their dispersion relation differs considerably:

$$\text{HE: } \omega = ck\,,$$
$$\text{SE: } \omega = k^2/2\,.$$

C.2. Definitions and Normalisation

According to (C.5) we define incoming and outgoing basis states:

$$\varphi_{\mathrm{l}}^{\mathrm{in}}(z,k) = \sqrt{\frac{1}{2ik}}e^{ik(z+l)}\,, \qquad \varphi_{\mathrm{l}}^{\mathrm{out}}(z,k) = \sqrt{\frac{1}{2ik}}e^{-ik(z+l)}\,,$$
$$\varphi_{\mathrm{r}}^{\mathrm{in}}(z,k) = \sqrt{\frac{1}{2ik}}e^{-ik(z-l)}\,, \qquad \varphi_{\mathrm{r}}^{\mathrm{out}}(z,k) = \sqrt{\frac{1}{2ik}}e^{ik(z-l)}\,,$$

where the index l stands for *left* and the index r stands for *right*.

The QNMs, according to our ansatz (C.1), are

$$\varphi_m(z) = \begin{cases} (-1)^m N_m e^{ik_m z} & z < -l \\ D_m e^{ik_m z} + (-1)^m e^{-ik_m z} & -l \le z \le l \\ N_m e^{ik_m z} & z > l \end{cases},$$

with the normalisation constant N_m. D_m is determined by the equation $\varphi_m(l^+) = \varphi_m(l^-)$:

$$D_m = -\frac{iN_m(ik_m - \gamma)}{k_m}\,.$$

In order to calculate the normalisation constant N_m from (C.6), we take some auxiliary steps by breaking down the surface term: first, since $\widetilde{\varphi}_m(k) = \sum_N \alpha_N \varphi_N^{\mathrm{out}}(k)$ where $\alpha_N = \left[\varphi_N^{\mathrm{in}} | \varphi_m\right]_{\partial V}$ (cf. [36] Equation (22)) and the linearity of the surface operator, the surface term becomes $\sum_N \alpha_N \beta_N$ with

$$\beta_{\mathrm{l/r}} := \left[\varphi_{\mathrm{l/r}}^{\mathrm{out}}(z,k_m)\left|\frac{\partial \varphi_{\mathrm{l/r}}^{\mathrm{out}}(z,k)}{\partial(k^2)}\right|_{k=k_m}\right]_{\mathrm{L/R}} = \frac{1}{4k_m^2}\,,$$

where L and R refer to the left and right 'surfaces'. Furthermore,

$$\alpha_{\mathrm{l}} = \left[\varphi_{\mathrm{l}}^{\mathrm{in}}(z,k_m)\middle|\varphi_m(z)\right]_{\mathrm{L}} = -\left(-1\right)^m N_m\sqrt{2ik_m}e^{ik_m l}\,,$$
$$\alpha_{\mathrm{r}} = \left[\varphi_{\mathrm{r}}^{\mathrm{in}}(z,k_m)\middle|\varphi_m(z)\right]_{\mathrm{R}} = -N_m\sqrt{2ik_m}e^{ik_m l}\,.$$

Substituting $\sum_N \alpha_N\beta_N$ into (C.6) yields:

$$\frac{\alpha_{\mathrm{r}}^2+\alpha_{\mathrm{l}}^2}{4k_m^2} + \int_{-l}^{l}\varphi_m(z)\frac{\partial(k^2\varepsilon(z,k))}{\partial(k^2)}\varphi_m(z)\mathrm{d}z = \frac{\alpha_{\mathrm{r}}^2+\alpha_{\mathrm{l}}^2}{4k_m^2} + \int_{-l}^{l}\varphi_m^2(z)\mathrm{d}z \overset{!}{=} 1\,,$$

from which we obtain N_m^2:

$$N_m^2 = \frac{(-1)^m k_m^2}{2\left(k_m+i\gamma\right)^2 L + 2ik_m - 2\gamma}\,. \tag{C.7}$$

C.3. Residues

The residues $\mathcal{R}_m$ are derived analogously to [36], however, with an additional factor $\frac{1}{2k_m}$:

$$\mathcal{R}_{m,NN'} = -\frac{1}{2k_m}\left[\varphi_N^{\mathrm{in}}(z,k_m)|\varphi_m(z)\right]_N\left[\varphi_m(z)|\varphi_{N'}^{\mathrm{in}}(z,k_m)\right]_{N'}\,. \tag{C.8}$$

It turns out that Green's second identity, which is used for the derivation of (C.8), does not hold for the 1DFP because neither ε nor φ_m are once or twice continuously differentiable. Consequently, we have to resort to the form of the residues given in [36], Equation (26):

$$\mathcal{R}_{m,NN'} = -\frac{1}{2k_m}\underbrace{\left[\varphi_N^{\mathrm{in}}(z,k_m)|\varphi_m(z)\right]_N}_{=\alpha_N}\langle\varphi_m(z)\left|\Delta\varepsilon(z,k_m)k_m^2\right|\varphi_{N'}^{\mathrm{bg}}(z,k_m)\rangle_{\mathcal{V}}\,. \tag{C.9}$$

Here $\Delta\varepsilon(z) = -\frac{2V(z)}{k^2}$, where $\varepsilon = \varepsilon_{\mathrm{bg}} + \Delta\varepsilon(z)$ is the deviation of the dielectric function from the background in which the scatterer is embedded; in our case vacuum, i.e., $\varepsilon_{\mathrm{bg}} = 1$.

Now we choose $\varphi_{N'}^{\mathrm{bg}}(z,k_m)$ to be an incoming plane wave from either the left, i.e., $N' = \mathrm{l}$ or from the right, i.e., $N' = \mathrm{r}$. This yields:

$$\langle\varphi_m(z)\left|\Delta\varepsilon(z,k_m)k_m^2\right|\varphi_{N'}^{\mathrm{bg}}(z,k_m)\rangle_{\mathcal{V}} = \begin{cases} -N_m\gamma\sqrt{-\frac{2i}{k_m}}e^{ik_mL/2}\left(\left(-1\right)^m + e^{ik_mL}\right) & N' = \mathrm{l} \\ -N_m\gamma\sqrt{-\frac{2i}{k_m}}e^{ik_mL/2}\left(-1\right)^m\left(\left(-1\right)^m + e^{ik_mL}\right) & N' = \mathrm{r} \end{cases}. \tag{C.10}$$

Finally, by substituting (C.10) into (C.9) and by utilising (C.2) for simplification, we arrive at

$$\mathcal{R}_m = -N_m^2 \left(i + k_m/\gamma\right) \begin{pmatrix} 1 & (-1)^m \\ (-1)^m & 1 \end{pmatrix} .$$

C.4. Background Through the Mittag-Leffler Expansion

So far the Mittag-Leffler Expansion (MLE) appeared only in (C.4) for the Green's function with which we derived the normalisation of the QNMs and the analytical residues of the S-matrix. In order to find the analytical background $S_{\mathrm{bg}}(k)$, we employ the MLE again, but this time on the analytical S-matrix itself.

Generally, the MLE for a meromorphic function $f(k)$ with poles k_m takes the form

$$f(k) = f(0) + f'(0)k + ... + \frac{f^{(p)}(0)}{p!}k^p + \sum_m \frac{\mathcal{R}_m (k/k_m)^{p+1}}{k - k_m} , \qquad \text{(C.11)}$$

where we define the order of the MLE to be $p+1$. An MLE of so-called zeroth order consists only of the sum-over-m part of (C.11); Equation (C.4) would be such an example disregarding the factor $\frac{1}{2k_m}$. Also, notice that the MLE assumes the form of a truncated Taylor expansion plus a pole term. We can split the sum over m by a partial fraction decomposition:

$$\sum_m \frac{\mathcal{R}_m (k/k_m)^{p+1}}{k - k_m} = \underbrace{\frac{...}{k_m^{p+1}}}_{\text{rest}} + \underbrace{\sum_m \frac{\mathcal{R}_m}{k - k_m}}_{\text{resonant term}} , \qquad \text{(C.12)}$$

where the second term on the right-hand side is the *resonant* part, while the truncated Taylor series plus the rest of the partial fraction decomposition constitute the *background* term.

In the previous sections we already derived the k_m and the residues $\mathcal{R}_m$. Thus, we know the resonant part of $S(k)$. All that is left to do is to determine the background and its required order. We obtain $S(0)$ and its derivatives from the analytical solution, cf. (B.2) and (B.3):

$$t(k) = \frac{k^2}{\gamma^2 \left(e^{2iLk} - 1\right) + k^2 + 2i\gamma k} ,$$
$$r(k) = -\frac{i\gamma k \left(e^{2iLk} + 1\right) + \gamma^2 \left(e^{2iLk} - 1\right)}{\gamma^2 \left(e^{2iLk} - 1\right) + k^2 + 2i\gamma k} .$$

The order can be determined by examining the asymptotic behaviour $|k| \to \infty$[3] of the transmission and reflection. For the 1DFP it turns out that we need an MLE of first order for the transmission entries in our S-matrix while the reflection entries require an MLE of third order.

Hence, we see from (C.11) and (C.12) that the background terms are

$$t_{\mathrm{bg}} = t(0) + \sum_m \frac{\mathcal{R}_{m,\mathrm{lr}}}{k_m}\,, \tag{C.13}$$

$$r_{\mathrm{bg}}(k) = r(0) + \partial_k r(0) k + \partial_k^2 r(0) k^2/2 + \sum_m \frac{\left(k_m^2 + k\,k_m + k^2\right)\,\mathcal{R}_{m,\mathrm{ll}}}{k_m^3}, \tag{C.14}$$

where $\partial_k^p r(0) \coloneqq \left(\frac{\mathrm{d}^p r(k)}{\mathrm{d}k^p}\right)(0)$ and

$$\begin{aligned} t(0) &= 0\,, \\ r(0) &= -1\,, \\ \partial_k r(0) &= -\frac{2\,i\,\gamma\,L + i}{2\,\gamma^2\,L + 2\,\gamma}\,, \\ \partial_k^2 r(0) &= \frac{2\,L^2\,\gamma^2 + 2\,L\,\gamma + 1}{2\,\gamma^2\,\left(L\,\gamma + 1\right)^2}\,. \end{aligned}$$

C.5. Final Expression and Results

The S-matrix expanded via Weiss' formalism is

$$S(k) = \begin{pmatrix} r_{\mathrm{bg}}(k) & t_{\mathrm{bg}} \\ t_{\mathrm{bg}} & r_{\mathrm{bg}}(k) \end{pmatrix} - \sum_m N_m^2\,\left(i + k_m/\gamma\right) \begin{pmatrix} (-1)^m & 1 \\ 1 & (-1)^m \end{pmatrix}\,.$$

The expressions for r_{bg} as well as t_{bg} are given in Equations (C.13)-(C.14), while N_m is given in (C.7). For a discussion of the results see Section 4.3.5.

[3] In fact, k must be sent infinitely far away from all poles. The resonant term in (C.11) will then vanish and all that is left is the polynomial part.

Bibliography

[1] M. Horodynski, M. Kühmayer, A. Brandstötter, K. Pichler, Y. V. Fyodorov, U. Kuhl, and S. Rotter, "Optimal wave fields for micromanipulation in complex scattering environments," *Nature Photonics* (Nov, 2019) . http://dx.doi.org/10.1038/s41566-019-0550-z.

[2] D. Bouchet, S. Rotter, and A. P. Mosk, "Maximum information states for coherent scattering measurements," 2020.

[3] K. Pichler, M. Kühmayer, J. Böhm, A. Brandstötter, P. Ambichl, U. Kuhl, and S. Rotter, "Random anti-lasing through coherent perfect absorption in a disordered medium," *Nature* **567** no. 7748, (Mar, 2019) 351–355. http://dx.doi.org/10.1038/s41586-019-0971-3.

[4] G. Breit and E. Wigner, "Capture of Slow Neutrons," *Physical Review* **49** no. 7, (Apr, 1936) 519–531. http://dx.doi.org/10.1103/physrev.49.519.

[5] W. Heisenberg, "Diebeobachtbaren Größen in der Theorie der Elementarteilchen," *Zeitschrift für Physik* **120** no. 7-10, (Jul, 1943) 513–538. http://dx.doi.org/10.1007/bf01329800.

[6] C. Mahaux and H. A. Weidenmüller, *Shell-Model Approach to Nuclear Reactions*. North-Holland, Amsterdam, 1969.

[7] S. Datta, "Electronic Transport in Mesoscopic Systems,". http://dx.doi.org/10.1017/cbo9780511805776.

[8] C. F. B. D. R. Huffman, *Absorption and Scattering of Light by Small Particles*. John Wiley & Sons, Ltd, 2007. https://onlinelibrary.wiley.com/doi/abs/10.1002/9783527618156.

[9] M. Åbom, "Measurement of the scattering-matrix of acoustical two-ports," *Mechanical Systems and Signal Processing* **5** no. 2, (Mar, 1991) 89–104. http://dx.doi.org/10.1016/0888-3270(91)90017-y.

[10] S. M. Popoff, G. Lerosey, R. Carminati, M. Fink, A. C. Boccara, and S. Gigan, "Measuring the Transmission Matrix in Optics: An Approach to the Study and Control of Light Propagation in Disordered Media," *Physical Review Letters* **104** no. 10, (Mar, 2010) . http://dx.doi.org/10.1103/physrevlett.104.100601.

[11] A. P. Mosk, A. Lagendijk, G. Lerosey, and M. Fink, "Controlling waves in space and time for imaging and focusing in complex media," *Nature Photonics* **6** no. 5, (May, 2012) 283–292. http://dx.doi.org/10.1038/nphoton.2012.88.

[12] A. Brandstötter, A. Girschik, P. Ambichl, and S. Rotter, "Shaping the branched flow of light through disordered media," *Proceedings of the National Academy of Sciences* **116** no. 27, (Jun, 2019) 13260–13265. http://dx.doi.org/10.1073/pnas.1905217116.

[13] R. Carminati, J. J. Sáenz, J.-J. Greffet, and M. Nieto-Vesperinas, "Reciprocity, unitarity, and time-reversal symmetry of theSmatrix of fields containing evanescent components," *Physical Review A* **62** no. 1, (Jun, 2000) . http://dx.doi.org/10.1103/physreva.62.012712.

[14] R. Carminati, M. Nieto-Vesperinas, and J.-J. Greffet, "Reciprocity of evanescent electromagnetic waves," *Journal of the Optical Society of America A* **15** no. 3, (Mar, 1998) 706. http://dx.doi.org/10.1364/josaa.15.000706.

[15] L. Deák and T. Fülöp, "Reciprocity in quantum, electromagnetic and other wave scattering," *Annals of Physics* **327** no. 4, (Apr, 2012) 1050–1077. http://dx.doi.org/10.1016/j.aop.2011.10.013.

[16] P. Ambichl, A. Brandstötter, J. Böhm, M. Kühmayer, U. Kuhl, and S. Rotter, "Focusing inside Disordered Media with the Generalized Wigner-Smith Operator," *Physical Review Letters* **119** no. 3, (Jul, 2017) . http://dx.doi.org/10.1103/physrevlett.119.033903.

[17] P. Ambichl, "Delay times and beam-like scattering states in coherent wave transmission through resonators," 2012.

[18] S. Rotter, J.-Z. Tang, L. Wirtz, J. Trost, and J. Burgdörfer, "Modular recursive Green's function method for ballistic quantum transport," *Phys. Rev. B* **62** (Jul, 2000) 1950–1960. https://link.aps.org/doi/10.1103/PhysRevB.62.1950.

[19] R. M. More, "Theory of Decaying States," *Physical Review A* **4** no. 5, (Nov, 1971) 1782–1790. http://dx.doi.org/10.1103/physreva.4.1782.

[20] R. M. More and E. Gerjuoy, "Properties of Resonance Wave Functions," *Physical Review A* **7** no. 4, (Apr, 1973) 1288–1303. http://dx.doi.org/10.1103/physreva.7.1288.

[21] R. Olshansky, "Propagation in glass optical waveguides," *Reviews of Modern Physics* **51** no. 2, (Apr, 1979) 341–367. http://dx.doi.org/10.1103/revmodphys.51.341.

[22] S. G. Tikhodeev, A. L. Yablonskii, E. A. Muljarov, N. A. Gippius, and T. Ishihara, "Quasiguided modes and optical properties of photonic crystal slabs," *Physical Review B* **66** no. 4, (Jul, 2002) . http://dx.doi.org/10.1103/physrevb.66.045102.

[23] S. Datta, "Level broadening," *Quantum Transport: Atom to Transistor* 183–216. http://dx.doi.org/10.1017/cbo9781139164313.009.

[24] T. Weiss, M. Schäferling, H. Giessen, N. A. Gippius, S. G. Tikhodeev, W. Langbein, and E. A. Muljarov, "Analytical normalization of resonant states in photonic crystal slabs and periodic arrays of nanoantennas at oblique incidence," *Physical Review B* **96** no. 4, (Jul, 2017) . http://dx.doi.org/10.1103/physrevb.96.045129.

[25] E. A. Muljarov and T. Weiss, "Resonant-state expansion for open optical systems: generalization to magnetic, chiral, and bi-anisotropic materials," *Optics Letters* **43** no. 9, (Apr, 2018) 1978. http://dx.doi.org/10.1364/ol.43.001978.

[26] P. Lalanne, W. Yan, K. Vynck, C. Sauvan, and J.-P. Hugonin, "Light Interaction with Photonic and Plasmonic Resonances," *Laser & Photonics Reviews* **12** no. 5, (2018) 1700113, https://onlinelibrary.wiley.com/doi/pdf/10.1002/lpor.201700113. https://onlinelibrary.wiley.com/doi/abs/10.1002/lpor.201700113.

[27] E. S. C. Ching, P. T. Leung, A. Maassen van den Brink, W. M. Suen, S. S. Tong, and K. Young, "Quasinormal-mode expansion for waves in open systems," *Reviews of Modern Physics* **70** no. 4, (Oct, 1998) 1545–1554. http://dx.doi.org/10.1103/revmodphys.70.1545.

[28] "The Dispersion Formula for Nuclear Reactions," *Proceedings of the Royal Society of London. Series A. Mathematical and Physical Sciences* **166** no. 925, (1938) 277–295. https://doi.org/10.1098/rspa.1938.0093.

[29] I. Rotter, "Dynamics of quantum systems," *Physical Review E* **64** no. 3, (Aug, 2001) . http://dx.doi.org/10.1103/physreve.64.036213.

[30] H. E. Türeci, A. D. Stone, and B. Collier, "Self-consistent multimode lasing theory for complex or random lasing media," *Phys. Rev. A* **74** (Oct, 2006) 043822. https://link.aps.org/doi/10.1103/PhysRevA.74.043822.

[31] J. Bang, F. Gareev, M. Gizzatkulov, and S. Goncharov, "Expansion of continuum functions on resonance wave functions and amplitudes," *Nuclear Physics A* **309** no. 3, (Oct, 1978) 381–421. http://dx.doi.org/10.1016/0375-9474(78)90488-8.

[32] G. B. Arfken and H. J. Weber, eds., *Mathematical Methods for Physicists*. Elsivier, London, sixth edition ed., 2011. http://www.sciencedirect.com/science/article/pii/B9780123846549000323.

[33] V. Grigoriev, A. Tahri, S. Varault, B. Rolly, B. Stout, J. Wenger, and N. Bonod, "Optimization of Resonant Effects in Nanostructures Via Weierstrass Factorization," *Physical Review A* **88** no. 1, (2013) 011803. https://doi.org/10.1103/physreva.88.011803.

[34] F. Alpeggiani, N. Parappurath, E. Verhagen, and L. Kuipers, "Quasinormal-mode expansion of the scattering matrix," *Physical Review X* **7** no. 2, (2017) . http://dx.doi.org/10.1103/physrevx.7.021035.

[35] F. Salihbegovic, "Reconstructing the Scattering Matrix Using the Quasi-Bound States," Master's thesis, TU Wien, 2018.

[36] T. Weiss and E. A. Muljarov, "How to calculate the pole expansion of the optical scattering matrix from the resonant states," *Physical Review B* **98** no. 8, (Aug, 2018) . http://dx.doi.org/10.1103/physrevb.98.085433.

[37] D. C. Brody, "Biorthogonal quantum mechanics," *Journal of Physics A: Mathematical and Theoretical* **47** no. 3, (Dec, 2013) 035305. http://dx.doi.org/10.1088/1751-8113/47/3/035305.

[38] W. Suh, Z. Wang, and S. Fan, "Temporal coupled-mode theory and the presence of non-orthogonal modes in lossless multimode cavities," *IEEE Journal of Quantum Electronics* **40** no. 10, (Oct, 2004) 1511–1518. http://dx.doi.org/10.1109/jqe.2004.834773.

[39] S. Rotter and S. Gigan, "Light fields in complex media: Mesoscopic scattering meets wave control," *Reviews of Modern Physics* **89** no. 1, (Mar, 2017) . http://dx.doi.org/10.1103/revmodphys.89.015005.

[40] W. Domcke, "Projection-operator approach to potential scattering," *Physical Review A* **28** no. 5, (Nov, 1983) 2777–2791. http://dx.doi.org/10.1103/physreva.28.2777.

[41] R. G. Newton, "Analytic Properties of Radial Wave Functions," *Journal of Mathematical Physics* **1** no. 4, (Jul, 1960) 319–347. http://dx.doi.org/10.1063/1.1703665.

[42] R. Colom, R. McPhedran, B. Stout, and N. Bonod, "Modal expansion of the scattered field: Causality, nondivergence, and nonresonant contribution," *Physical Review B* **98** no. 8, (Aug, 2018) . http://dx.doi.org/10.1103/physrevb.98.085418.

[43] E. A. Muljarov, W. Langbein, and R. Zimmermann, "Brillouin-Wigner perturbation theory in open electromagnetic systems," *EPL (Europhysics Letters)* **92** no. 5, (Dec, 2010) 50010. http://dx.doi.org/10.1209/0295-5075/92/50010.

[44] M. B. Doost, W. Langbein, and E. A. Muljarov, "Resonant state expansion applied to two-dimensional open optical systems," *Physical Review A* **87** no. 4, (Apr, 2013) . http://dx.doi.org/10.1103/physreva.87.043827.

[45] E. A. Muljarov and W. Langbein, "Exact mode volume and Purcell factor of open optical systems," *Physical Review B* **94** no. 23, (Dec, 2016) . http://dx.doi.org/10.1103/physrevb.94.235438.

[46] S. V. Lobanov, G. Zoriniants, W. Langbein, and E. A. Muljarov, "Resonant-state expansion of light propagation in nonuniform waveguides," *Physical Review A* **95** no. 5, (May, 2017) . http://dx.doi.org/10.1103/physreva.95.053848.

[47] S. V. Lobanov, W. Langbein, and E. A. Muljarov, "Resonant-state expansion of three-dimensional open optical systems: Light scattering," *Physical Review A* **98** no. 3, (Sep, 2018) . http://dx.doi.org/10.1103/physreva.98.033820.

[48] S. Lobanov, W. Langbein, and E. Muljarov, "Resonant-state expansion applied to three-dimensional open optical systems: Complete set of static modes," *Physical Review A* **100** no. 6, (Dec, 2019) . http://dx.doi.org/10.1103/physreva.100.063811.

[49] T. Weiss, N. A. Gippius, S. G. Tikhodeev, G. Granet, and H. Giessen, "Derivation of plasmonic resonances in the Fourier modal method with adaptive spatial resolution and matched coordinates," *Journal of the Optical Society of America A* **28** no. 2, (Jan, 2011) 238. http://dx.doi.org/10.1364/josaa.28.000238.

[50] T. W. Gamelin, "Complex Analysis," *Undergraduate Texts in Mathematics* (2001) . http://dx.doi.org/10.1007/978-0-387-21607-2.

[51] H. Feshbach, "A unified theory of nuclear reactions. II," *Annals of Physics* **19** no. 2, (Aug, 1962) 287–313. http://dx.doi.org/10.1016/0003-4916(62)90221-x.

[52] J. Humblet and L. Rosenfeld, "Theory of nuclear reactions," *Nuclear Physics* **26** no. 4, (Sep, 1961) 529–578. http://dx.doi.org/10.1016/0029-5582(61)90207-3.

[53] T. Berggren, "Completeness relations, Mittag-Leffler expansions and the perturbation theory of resonant states," *Nuclear Physics A* **389** no. 2, (Nov, 1982) 261–284. http://dx.doi.org/10.1016/0375-9474(82)90519-x.

[54] T. Berggren and P. Lind, "Resonant state expansion of the resolvent," *Physical Review C* **47** no. 2, (Feb, 1993) 768–778. http://dx.doi.org/10.1103/physrevc.47.768.

[55] A. Peña, A. Girschik, F. Libisch, S. Rotter, and A. A. Chabanov, "The single-channel regime of transport through random media," *Nature Communications* **5** no. 1, (Mar, 2014) . http://dx.doi.org/10.1038/ncomms4488.

[56] K. Özdemir, S. Rotter, F. Nori, and L. Yang, "Parity–time symmetry and exceptional points in photonics," *Nature Materials* **18** no. 8, (Apr, 2019) 783–798. http://dx.doi.org/10.1038/s41563-019-0304-9.

[57] A. I. Kuznetsov, A. E. Miroshnichenko, M. L. Brongersma, Y. S. Kivshar, and B. Luk'yanchuk, "Optically resonant dielectric nanostructures," *Science* **354** no. 6314, (Nov, 2016) aag2472. http://dx.doi.org/10.1126/science.aag2472.

[58] H. Feshbach, "Unified theory of nuclear reactions," *Annals of Physics* **5** no. 4, (Dec, 1958) 357–390. http://dx.doi.org/10.1016/0003-4916(58)90007-1.

[59] J. R. Taylor, *Scattering theory: the quantum theory of nonrelativistic collisions*. Courier Corporation, 2006.

[60] S. Rotter, "A modular recursive Green's function method for quantum transport," 1999.

[61] A. Maignan and T. Scott, "Fleshing out the Generalized Lambert W Function," *ACM Communications in Computer Algebra* **50** no. 2, (June, 2016) 45–60. https://hal.archives-ouvertes.fr/hal-01326771.

Appendix D.

Attachments

Attached to this pdf are three zip-archives.

- `complex-waveguide-code-and-data.zip`: Python code implementing Salihbegović's and Alpeggiani's reconstruction as well as most of the plots of this work as well as the raw QNM data (far-fields + complex energies) for the complex waveguide.

- `1dfp.zip`: Maxima code that was used for calculating the analytical expressions of Weiss' formalism and corresponding python code for the numerical implementation of the 1DFP.

- `blender-files.zip`: Blender files used for plotting the 3D visualisation of the waveguide (Figure 4.1). It also contains a file with the Teflon scatterer positions.

Hiermit erkläre ich, dass die vorliegende Arbeit gemäß dem Code of Conduct – Regeln zur Sicherung guter wissenschaftlicher Praxis (in der aktuellen Fassung des jeweiligen Mitteilungsblattes der TU Wien), insbesondere ohne unzulässige Hilfe Dritter und ohne Benutzung anderer als der angegebenen Hilfsmittel, angefertigt wurde. Die aus anderen Quellen direkt oder indirekt übernommenen Daten und Konzepte sind unter Angabe der Quelle gekennzeichnet. Die Arbeit wurde bisher weder im In– noch im Ausland in gleicher oder in ähnlicher Form in anderen Prüfungsverfahren vorgelegt.

Wien, am Unterschrift